Lawrence Berkeley National Laboratory
Recent Work

Title
Microclimate Effects near the Ground in the Suburban Environment

Permalink
https://escholarship.org/uc/item/0tp0w6qf

Author
Smith, C.K.

Publication Date
1996-07-01

ERNEST ORLANDO LAWRENCE BERKELEY NATIONAL LABORATORY

Microclimate Effects Near the Ground in the Suburban Environment

C.K. Smith, S. Bretz, and H. Akbari
Energy and Environment Division

July 1996

DISCLAIMER

Microclimate Effects Near the Ground in the Suburban Environment

Craig K. Smith, Sarah Bretz, and Hashem Akbari

Heat Island Project
Energy & Environment Division
Lawrence Berkeley National Laboratory
University of California
Berkeley, CA 94720

July 1996

Table of Contents

List of Tables

iii

List of Figures

MICROCLIMATE EFFECTS NEAR THE GROUND
IN THE SUBURBAN ENVIRONMENT

Craig Kenton Smith†, Sarah Bretz, and Hashem Akbari
Heat Island Project
Energy and Environment Division
Lawrence Berkeley National Laboratory
Berkeley, CA 94720

Abstract

We performed an experiment to monitor the ambient air temperature at 18 locations around a suburban residence, from which we have identified the influence of a variety of microclimate effects. A spatial average temperature, T_{ave}, was computed from 13 of these locations, and the difference between the temperature at each sensor and the average is taken as a measure of the microclimate variation. For each location, the temperature difference follows a diurnal pattern characteristic of the local environment. Generally, locations in proximity to the structure exhibit a daytime peak while those adjacent to shade trees show a daytime trough in their diurnal patterns. A third pattern containing both of these features can occur in locations where a competition between heating and cooling influences takes place. The size of peaks and troughs can be a large as 2-3 °C on a warm day at the site (25 °C). The night-time value of the temperature difference is also determined by features in the local environment which govern long wave radiative losses.

Regressions of the daily extrema of the temperature difference against the daily maximum T_{ave} shows that microclimate effects usually become more influential on warmer days. We found that an increase in the average site temperature by 10 degrees results in a change of a few tenths to one degree in the daytime extrema. The same type of regression analysis was applied to the temperature difference and the spatial average temperature, both taken at the time of maximum of T_{ave}. As the difference data rarely shows an extremum at this time, the correlations are in some instances weaker, but generally show the same trends.

While the results of the analysis are site specific, they indicate the difficulty in finding locations near the ground in the suburban environment where these microclimate effects are minimized, and where accurate measurements of a site or neighborhood representative temperature can be made.

---

†   Currently PO Box 1881, El Cerrito, CA 94530

MICROCLIMATE EFFECTS NEAR THE GROUND
IN THE SUBURBAN ENVIRONMENT

Craig Kenton Smith, Sarah Bretz, and Hashem Akbari

I. Introduction

A. The Need for Suburban Microclimate Measurement

Field monitoring and computer simulations have demonstrated that cooling energy use for individual buildings can be reduced significantly through the use of shade trees and high albedo roofing materials (Taha, 1988; Akbari et al., 1993, 1995). Such strategies also lower the amount of solar energy converted to sensible heat in the environment (Oke, 1978), reducing outdoor air temperatures. Meteorological simulations indicate they can result in an indirect or neighborhood-wide cooling effect if employed over a large enough area (Taha et al., 1988). Thus, the indirect cooling effects of shade trees and high albedo surfaces show great potential for reducing urban heat islands in the summer (Akbari et al., 1990; Kurn et al, 1994).

Building energy simulation programs such as DOE 2.1 are used to predict the cooling load reduction for a variety of structures subjected to indirect effects (Huang et al., 1987; Taha et al., 1988). Such simulations require as input climate data for the region. Indirect effects are included as a reduction in ambient air temperature below the urban canopy, and the energy savings is given as the difference between the cooling energy consumption with and without this reduction.

For example, to model the effect of changing the density of tree cover over a neighborhood on residential cooling energy use, the reduction in air temperature must be known as a function of the density (and type) of neighborhood trees. Estimates of neighborhood temperature reduction can be made from the published maximum evapotranspiration rates for different types of vegetation and the volume of air with which the cool air is mixed, per unit time (Huang et al., 1987), but this method is problematic for several reasons. While the maximum rate of evapotranspiration is known as a function of ambient temperature and insolation for a variety of crops and some trees (see for example Jensen and Haise, 1963), it is by no means known for all types of trees and other vegetation encountered in the urban environment. In addition, use of these rates will tend to overestimate evapotranspiration for sites that are not well watered. Also uncertain is the degree of mixing of the cool with the local air and the mixing height (Huang et al., 1987).

Similarly, numerical climate models used to predict the influence of albedo suffer from uncertainties which make accurate determination of the below canopy temperature difference difficult (Sailor, 1993). It is therefore important that these theoretical estimates and simulation results of temperature reduction be compared with the results of experiments carried out under actual conditions in the urban or suburban environment. Typically, such experiments focus on neighborhood air temperature as a function of the density of vegetative cover.

To assess the relationship between urban climate and the density of tree cover, Sailor et al. (1992) examined 50 summer days of temperature data from 15 residential sites of varying neighborhood tree cover, scattered around Sacramento. Temperature data were collected by automated weather stations installed at a height of 1 meter in the back yards of the sites. While they attempted to minimize biases coming from other gross differences between the neighborhoods-- albedo, building density, and substrate properties, no attempt was made to measure these parameters, known to be important in determining local meteorology (Atwater, 1972). On a smaller scale, weather stations were placed as far as possible from obvious obstructions to wind flow, but specific site characteristics which could cause microclimate variations in the vicinity of the weather stations were not identified nor taken into account: these include the placement of structures, fences, trees and various surfaces (pavement, ground cover, water or bare dirt). Biases from these sources may have resulted in the anomalously wide spread observed in the time of maximum temperature between the sites, and contributed to the inability of the experiment to detect a correlation between the temperature maxima and the density of tree cover.

Kurn et al. (1994) performed a series of traverse measurements of air temperature and relative humidity over a sodded section of Whittier Narrows Recreation Area, a residential park in Southern California. They found that air temperatures in the park were lowered by 1-2 °C relative to that found on city streets near the park. But the large variation in temperature they saw along the traverse inside the park shows the influence of other microclimate effects, most likely resulting from nearby trees and parking lots, were probably was not negligible.

McGinn (1982) realized the importance of site specific characteristics in his study of the microclimate effects[1] of neighborhood tree cover in Sacramento, and attempted to minimize their influence by choosing measurement locations which were not believed to be unduly influenced by a single element in the environment. Some general criteria, such as placing instrumentation out of the immediate wind shadow of local structures, and away from locations "completely sheltered by a large tree," were followed as much as the restrictions on available sites allowed. But without performing an analysis of the microclimate variation around each site first, it was not possible to know the combined effect of all site elements at the measurement points.

Realizing that proximity to trees and buildings was inevitable at most suburban sites, Heisler et al. (1994) took a different approach in their attempt to quantify the influence of Chicago's urban forests on the climate in residential neighborhoods. In their initial analysis, they determined "morphology descriptors" related to the amount of sky blocked by local buildings and trees at 4 of their measurement points. To quantify the relationship between site morphology and wind reduction, various mathematical models were fit to the data in order to find a formula which adequately predicts the change in wind speed (relative to a local airport) as a function of the morphological descriptors. In the full analysis, models will be developed to predict the effect of site morphology on local air temperatures as well.

---

[1] The distance scale often implied by the word "microclimate" is on the order of 100m or larger. In this paper, however, we are concerned with variations on a much smaller scale, generally on the order of ten meters or less.

Clearly, more than the gross properties of a neighborhood (average albedo, building height, density, and substrate properties) must be considered in the siting of climate sensors in experiments to determine the magnitude of indirect cooling effects. Local properties around the measurement point can cause microclimate variations which systematically bias the temperature measurements. Near ground (below canopy) temperatures in the urban or suburban environment are known to be strongly influenced by factors such as sky view, surface moisture, reflectivity and emissivity of individual objects, shading, and advection. Structures, fences, windbreaks, paved surfaces or tall vegetation--and their orientation relative to the solar path and to each other--can result in large microclimate variations over very small scales (McGinn, 1982). Given the relatively small differences in air temperature between neighborhoods that one seeks to observe, the measurement points must either be located in similar microclimates, or placed where the effect of microclimate variations on the measurement is minimized. For measurements conducted near the ground, microclimate variations on the scale of individual roughness elements must therefor be considered.

Understanding the magnitude and daily pattern of microclimate variations that can occur in the suburban or urban environment is important, for several reasons. First, as illustrated above, one would like to identify locations which minimize very localized microclimate variations near the ground in the urban or suburban environment. Conversely, understanding the microclimate variation as a function of site properties allows one to go from the gross neighborhood picture of climate variables to a household (or smaller) scale picture of the microclimate, useful to landscape architects and others concerned with the thermal comfort conditions in the urban or suburban environment.

B. Overview

1. The Experiment

To identify and analyze the microclimate variations and their sources in the suburban environment, we performed an experiment in September-November 1994 to measure the ambient air temperature at 18 points around a large suburban lot containing an inhabited residence. In addition to a house, the property has many of the features one would expect to find in a suburban community and is therefore well suited for this type of experiment. We concentrated on the air temperature around these features, and over several relatively open areas with various surfaces.

From the data, we construct a spatial average temperature for the site as a function of time. The difference between the temperature at each measurement point and the spatial average is considered to be a good measure of the microclimate variation at that point. We first characterize the basic types of diurnal profiles seen in the temperature difference data, then examine in detail the profile for each sensor and correlate it with the properties of the local environment. That is, we attempt to identify the influence that each of these features has on the local microclimate. Finally, we correlate the size of the microclimate effects present during daylight hours with the daily maximum of the spatial average temperature.

2. Hypotheses of the Experiment

In designing our experiment, we formulated the following hypotheses for testing:

(1) There exist microclimate effects in the suburban environment which can cause the ambient air temperature to vary significantly around a residential lot during the day.

(2) There exists a correlation between microclimate and site morphology around the measurement point, such as the placement of structures, roads, shade trees, etc., and their orientation with respect to the solar path and each other. Specifically, the diurnal pattern of the temperature difference from the spatial average should be a predictable (at least qualitatively) function of the surrounding environment.

(3) The size of the resultant temperature variations are correlated with the (spatial) average ambient air temperature.

As an example of the application of these hypotheses to a particular site morphology, consider a shade tree surrounded by short grass, far from any structures. We expect:

(1) The ambient air temperature at chest height (1.5m) under and around the shade tree will be significantly cooler during the day and possibly warmer during the night than an equivalent area without trees.

(2) The daytime temperature depression results from two microclimate effects: shading of the ground, and the increased share of evapotranspiration (reduced sensible heat) in the local surface energy budget. Night-time temperature elevation may occur because surfaces under the tree are not able radiate to the sky as effectively as open locations.

(3) The minimum of the temperature depression should show a high negative correlation with the maximum (spatial average) ambient air temperature, because evapotranspiration from the tree is an increasing function of both air temperature and solar input.

We will also attempt to find any areas around the site where one can measure an air temperature which is negligibly influenced by local microclimate effects, and if so, how far from the microclimate effect producing elements of the site a sensor must be to obtain this result.

II. Experimental Design

A. The Site and Sensor Distribution

The site for our experiment is located in Lafayette California, 12 km due east of the Lawrence Berkeley National Laboratory and the UC Berkeley campus. The summer and early fall climate tends to be dry, with daytime maximum temperatures in the range of 20-32 °C. Lafayette is mostly isolated from the marine breeze circulation, which cools much of the Bay Area, by the Berkeley Hills to the west. An important mesoscale factor in the climate during summer and fall months is the air flow that results from differential heating from the central valley to the coast of California. As air in the central valley warms and rises in the morning, coastal air is pushed toward the Central Valley by the resulting pressure gradient. During the night, the reverse process occurs: the Central Valley cools faster than the coast. Thus, winds generally blow from the west during daylight hours, and from the east at night.

In addition to a residence, the experiment site has many of the features one would expect to find in a suburban community: a windbreak, swimming pool, small orchard, courtyard, clearing, driveway, carport, open and enclosed patios, large and small trees, ground cover and other types of vegetation.

Figure 1a shows a layout of the experiment site and 1b the locations of the sensors, numbered 1-18. Initially, we distributed twenty temperature sensors around the property, some near and some far from the features listed above. Two sensors (1,16) were placed in relatively open, unobstructed areas with little vegetation. Three sensors (4,5,7) were placed under or in tree canopy, and two (2,3) over and in a creek bed, with all far from structures. Six were under or adjacent to tree canopy, but near the house (7,11,13,14,15,19). Two others (6,10) were placed near the house but more distant from any significant vegetation. Most sensors were placed about 1.5m above the ground. Table 1 gives a description of the location and environment of each sensor.

Data from two of the temperature sensors were not used at all: 0, which was used to monitor the temperature inside the room of the house containing the data logger; and 12 (which did not have the proper construction).

The sensor above the roof (number 17) was attached to a weather station tower. Also attached to the tower were: a Campbell Scientific model 207 temperature and relative humidity probe, a Model 014A wind speed sensor, a Model 024A wind direction sensor, and a Model LI200S pyranometer (Li-Cor, repackaged by Campbell).

B. Temperature Sensor Construction

Each temperature sensor consisted of a single type T thermocouple inserted inside an aspirator. We custom designed aspirators to keep each thermocouple well shielded and ventilated. An aspirator consists of an insulating and reflective housing, and a small 12V DC fan (U.S. Toyo 402012MW) , which draws the ambient air through the housing and over the thermocouple (Figure 2).

The housing is constructed of one 15 cm and two 10 cm segments of white 3/4" PVC pipe, assembled into the shape of a "U" with two PVC elbows. The PVC pipe is covered in three sections of foam Armstrong Armaflex 25/50 hot water pipe insulation (R-6) which fit snugly over the entire surface.

A 4 mm hole in the PVC elbow nearest the fan allowed insertion of the thermocouple wire into the housing. A few inches of the stiff thermocouple wire behind the junction were curled into a helical shape and the tip was inserted through a stiff, large mesh screen to prevent the thermocouple from moving inside or dislodging from the housing. The housing was assembled, and the foam insulation was completely wrapped with aluminum tape[2]. A screen was fastened over the intake of the aspirator to prevent capture of windblown debris and insects.

---

[2] While a high IR emissivity covering would allow more efficient radiation of heat from the surface during the day, it would also allow the surface to be coupled by radiative exchange to sky and local surfaces at night, possibly

C. Data Collection Hardware

A length of the same type T thermocouple wire was used to connect the sensor to an Analog Devices μMac 5000 data logger residing in a bedroom of the house. The data logger recorded an entry for each sensor every 2.3 minutes. Each entry consisted of the average of 50 consecutive measurements taken an average of 2.7 seconds apart. Each measurement was integrated over 3 cycles of AC power (0.0500s) to eliminate the possibility of 60 Hz pickup in the long wires leading from the thermocouples to the logger. While open circuit voltages on the thermocouple wire ran typically in excess of 20 mV at 60Hz, an analog filter in the logger sent most of this signal to ground before integration.

Thermocouple wires were connected to connector blocks, each capable of accepting four thermocouple inputs, and each with its own AD590 temperature sensor, which is read alternately with the channels. Software compensation for the temperature of the thermocouple-block connection was performed using the data from the AD590s. A pull-up resistor in the logger set the voltage for unused channels at +5V; in this way, open circuits (broken thermocouples) could be detected by the logger; open connections resulted in a large integer (~9e07) being placed in the data stream.

The pyranometer and RH sensor were read by the same logger, without temperature compensation. Wind speed and direction sensors were read by another logger, but due to our programming error, the data could not be decoded into an azimuth and velocity of the correct magnitude, and thus could not be used.

Data from the main logger was recorded by an IBM XT computer. Data was manually put to floppy disk every few days, and taken to the laboratory for analysis.

III. Experimental Procedure

A. Data Collection

We collected temperature, humidity and insolation data from the first day of installation of the equipment on September 11, 1994. Over the next two weeks there were several failures of the thermocouple wires and junctions, which required replacement. The first data usable for our purposes was obtained on September 27 (Julian day 270), and data was collected continuously until the evening of November 18 (Julian day 322).

1. Thermocouple Failures and Redundancy

During the first two weeks of the data run (September 27 to October 6), several more thermocouple wires failed. We were relying on obtaining a calibration run at the end of the experiment, and we felt a thermocouple which was removed during the course of the experiment might not get calibrated. Therefore, thermocouples which failed after the first week were left in their

---

biasing the temperature measurements. It is therefore wise to use a covering with a high reflectivity but an intermediate value of the IR emissivity when taking night measurements.

6

channels, and another thermocouple was inserted into the same aspirator, and connected to a free channel on the data logger on October 6. This was the case with sensors 2, 14, and 17. The original thermocouple is designated "a", and the new, "b."

Other thermocouples failed intermittently during the experiment. This includes sensor 8, which showed an open circuit over several days in the last two weeks of the data run, and others which showed only one or two brief interruptions during the run. These failures were not found until after the run: no other "b" thermocouples were installed.

After October 6, we had 21 thermocouples (in 18 aspirators), 1 pyranometer, and 1 RH sensor connected to the principal data logger. No sensor/channel combinations were changed after this date.

B. Calibration

1. Design Check

During the development of the temperature sensors in July and August, checks were performed on each design to determine sensitivity to direct sunlight. Temperature measurements from two aspirated sensors of the same design, one shaded and one in full sun, were regressed separately against data from an adjacent, well ventilated and shaded bare thermocouple (the control). Comparison of the two regressions for the final design showed that the systematic offset from solar heating was at or less than 0.3 °C over the range of temperatures (0-30 °C) that would be encountered during the experiment. Calibration of each of the sensors used was performed after the data run.

2. Calibration Runs

While we tried several techniques for calibrating the sensors in air, none resulted in all 21 thermocouples, spread over a 2m by 1m area, being exposed to the same temperature simultaneously. The only successful calibration in this respect was a water immersion calibration, which required removing each thermocouple from its aspirator. The water calibration requires a set-up different from that of the experiment, and does not compensate for any variations in the aspirators. We believe this method gives satisfactory results as long as the aspirators are reasonably uniform in manufacture.

The calibration run was performed using a magnetically stirred water bath. Thermocouples were immersed in groups of 9 or 10 along with an immersion thermometer, one digital probe, and one thermocouple (7) which was made common to all groups. Data was logged briefly, only when the temperature of the immersed thermometers and thermocouples had stabilized. This process was repeated for six different temperatures between 0 and 55 °C. In the end, each group of thermocouples could be calibrated against thermocouple 7 and the two thermometers.

We selected the common thermocouple (7) to be used as the reference in calibrating the others, although the difference between it and the probe and immersion thermometer were not negligible (for example T(probe)= 1.32+ 1.02T(7)). The resolution of the probe and thermometer were

much larger than for the thermocouples (0.5 and 0.1°C respectively), and so we did not use them as the reference. Thus we perform an internal calibration on the temperature data. This will not significantly affect the following analysis, where we are mainly interested in temperature differences (see Section IV.B.5).

Linear regressions for each thermocouple against the selected thermocouple were performed to find calibration coefficients. All thermocouples showed linear behavior relative to the selected thermocouple, with no more than a 3% deviation from slope unity. All the regressions had $R^2 > 0.998$. The set of additive constants found in the calibration varied by over 3 °C. The reason for this is not all the AD590 temperature sensors (used for temperature compensation, see Section II.C.) were trimmed properly. Thus, these constants dominate the calibration equation, and the calibration of each sensor depends mainly on the channel to which it was connected.

3. Restoration of Broken Thermocouples

Several of the thermocouple junctions were found to be in poor condition when the aspirators were removed for the calibration (thermocouples 8,16,18). The junctions were resoldered, or the ends trimmed and new junctions were made, as needed. As the thermocouples were of the same T-type wire, we do not expect differences between the properties of the new and old junctions to be significant.

IV. Data Reduction for Analysis

A. Calibration of the Data

The data were filtered to remove spurious signals (replaced with white space in the data file) resulting from open circuit and short conditions, and then calibrated using the coefficients as determined above.

B. Time Averaging

In Figure 3 we show the calibrated data for five of the temperature sensors, as well as insolation and relative humidity, for the week of October 16 through 22 (Julian days 289 through 295). Although the week shown is in late October, the daily maximum temperatures generally run between 20 - 27 °C. Nightly minimum temperatures can be as low as 9 °C. This is typical of the fall climate in the Lafayette area.

For display purposes, the data in Figure 3 has been averaged over 0.01d (14.4 minute) intervals. Averaging over this period suppresses high frequency variability to the level that the overall diurnal pattern of temperature variation can be recognized.

The maximum number of data points averaged in each 0.01d interval is 6, and we insist there be at least three good values (non white space) in an interval for an average to be computed. Time averaging over 0.01d is used to produce data for all subsequent figures, and also in a later stage of the reduction.

C. Difference of Temperatures from Two Sensors

While the averaged data clearly shows the daily pattern of temperature at each location, it is difficult to see differences between locations other than gross features such as maxima and minima. The most obvious resolution of this problem is to compute and plot the difference between two channels as a function of time. One would clearly have to make a considerable number of difference computations and plots ($N*(N-1)/2=153$) in order to cover the entire data set this way. While such plots can demonstrate the existence of significant variations in temperature around the site, they only give information about the relative size of microclimate variations at two locations, not the magnitude or timing of these variations for individual locations.

D. Spatial Average of Temperature Sensors

1. Need for the Spatial Average

In order to determine the magnitude of microclimate effects at the location of each sensor, one would like, for comparison, a reference air temperature which is unbiased by these effects, i.e., temperature data taken away from the influences of small scale microclimate variations at the site. But, in this experiment, we did not measure any single temperature which is guaranteed to be free from local microclimate effects: all the measurements are being made near the ground, or in any case, far below the canopy of the tallest trees surrounding the site. Nor can we select, a priori, which sensor will give the most unbiased estimate of local temperature: to do so would assume an outcome for this experiment.

We must select a reference derived from the existing temperature data. Without further information, the most unbiased reference we can compute from the available data is the average over the temperature sensors. We refer to this as the spatial average temperature for the site.

2. Construction of the Average

In practice, we compute the spatial average, T_{ave}, using only those sensors that were operating continuously for the entire duration of the experiment (9/27 to 11/18; Julian days 270-322), excluding sensor 13 because of its offset problem (See Section V.C.1). We therefor chose (in counter clockwise order around the structure) sensors 1,3,4,5,6, 7,16,9,18,10, 11, 15, and 19 in computation of the average. We use calibrated data that is not time averaged.

E. Subtraction of the Average from the Temperature Data

Once we have the spatial average, the simplest way to compare it to the temperature data from one measurement point is to subtract it from that data. If the spatial average is not overly biased by the choice of sensors included, then the difference between temperature data for each location and the average should be a good measure of the microclimate effects at that location.

There was no guarantee that the average does not suffer from bias, due to both the temperature sensors selected to be in the average, and the effect of the large trees on the West and South Sides of the site. Once we establish the behavior of each sensor relative to the average, we will take up again the issue of this bias.

The spatial average was subtracted from the temperature data for each of the sensors, and the result was time averaged.[3] We refer to the time averaged difference data for one sensor as the "subtraction" or "difference" for that sensor. Plots of the spatial average and the subtractions are shown in Figure 4 for the same sensors and time interval as in Figure 3. The plots in the figure span the types behavior seen in the full set of subtractions.

The data for Sensor 13 shows an unusually large offset from the average, and we think this results from a problem with the calibration. We therefore will confine ourselves to analysis of the diurnal pattern for this sensor, and not place much emphasis on interpreting the absolute temperature values.

V. Analysis

A. Overview

The detection and analysis of microclimate effects around the experiment site is done using the subtractions. To test our hypotheses (Section I.B.2), we perform the following tasks in this section:

(1) Identify the diurnal pattern in the subtraction for each sensor location;

(2) Relate the diurnal patterns found to the site morphology (the objects around each sensor location and their orientation);

(3) Regress the daytime extrema of the temperature difference against the daily maximum air temperature, determined from the spatial average;

(4) Regress the temperature difference at the hottest point in the day against the air temperature at that time.

The last two tasks will correlate the magnitude of microclimate effects at each measurement location with the daily maximum temperature, as determined from the spatial average.

The events that we are trying to correlate under task 3 are not simultaneous. The extrema of the subtractions, dependent variables, often occur earlier than the maximum of the spatial average temperature, the independent variable. But, we are not trying to assert a causal relationship between the two. We are simply trying to find an indicator from which one could, given the local weather forecast, make a reasonable estimate of the magnitude of microclimate effects to be expected at the measurement points.

The forth task makes more conservative assumptions on the relationship between the magnitude of microclimate effects and the maximum daily temperature. Here, we examine the relationship between the two at the same instant, during the hottest time of the day. Unfortunately, we will find that the correlations are not as strong as those found in task (3), because at the time of

---

[3] The time averaging and subtraction operations do not commute because of the presence of gaps denoted as white space in the data. Time averaging the data before subtracting the average would cause data from different times to be subtracted whenever there was a gap in the data from one of the channels.

maximum average temperature, the temperature difference is usually not at its daytime extremum.

Note that the (daytime) extremum of the temperature difference is not synonymous with the maximum microclimate effect as the later is determined from absolute temperature differences rather than the signed differences calculated above.

B. The Diurnal Patterns of Temperature Variation around the Site

1. Existence of Diurnal Patterns for all Sensor Locations

Figure 4 clearly demonstrates that ambient air temperature varies significantly from location to location around the site. In addition, not one sensor shows a negligible difference (less than 0.3 °C) from the spatial average for more than a few hours. For these temperature differences to be considered the result of localized microclimate effects, it is necessary to show that they are regular in occurrence (e.g. follow a similar pattern each day), and that they correlate well with the surroundings of the measurement point.

Each of the subtractions in Figure 4 shows a pattern of peaks and valleys placed at about the same time every day. The amplitude and extremes of variation may change somewhat from day to day, but the basic pattern remains the same. The patterns become clearer when several days of data are overlaid in time and averaged (co- averaging). Figure 5 shows the *diurnal difference patterns* that result from co-averaging 15 days of subtraction data (Julian days 285 through 299).

For most sensor locations the diurnal pattern repeats for the entire duration of the experiment. The patterns for a few of the sensor locations begin to change in early November, when the climate pattern in Lafayette was changing from fall to winter conditions (but we will not examine the metamorphosis here).

2. Classification Scheme for Diurnal Patterns in Subtractions

On inspection, most of the diurnal difference patterns of Figure 5 consist of a significant daytime variation from a relatively constant night-time value. The difference patterns can be roughly classified into three major types, based on their daytime behavior: those which show (1) a significant peak, (2) significant trough, and (3) an oscillatory behavior, with both a significant peak and trough. A peak or trough is considered to occur during daytime if its extremum occurs between 7:30 a.m. and 5:30 p.m. PST, when the solar insolation value is not zero (Figure 6). When both daytime peaks and troughs occur, the most significant forms the basis for classification, unless they are of commensurate size (type 3).

The small scale lumpiness in the patterns (0.3°C or less) does not necessarily reflect real changes in air temperature difference at the same time each day: it can result from an anomalous distribution in the timing of peaks and valleys in the pattern over the 15 day period or from events such as the onset or retreat of shade around a sensor, which occurs at approximately the same time each day. Others may reflect actual changes in air temperature.

11

Difference patterns of the first type come from locations 1, 6, 9, 18, 10, 11, and 16. Sensors in locations 2, 3, 4, 5, 7, 8, 14, 15, 17, and 19 yield difference patterns of the second type. Location 13 exhibits a significant daytime trough and peak in rapid succession, and is therefore of type 3. While possible to further subdivide each class on the basis of the shape of the principal peak or trough, or the presence of other features, this will not be necessary for the quantitative analysis, where we focus only on the daytime extrema.

3. Daily Pattern of Insolation and Average Temperature

The diurnal patterns for insolation, relative humidity, and spatial average temperature were found by co-averaging over the same 15 day interval (Figure 6). As one would expect, the spatial average temperature begins to rise with insolation, but soon begins to lag behind it. The maximum spatial average temperature follows the maximum insolation by almost two hours. Over the course of the entire data run the average time of occurrence for both was:

$$t_{solar,max} = 11:52,$$

$$t_{T,max} = 13:43, PST.$$

The spatial average temperature begins to descend rapidly only after the insolation has dropped to 35% of its peak value, and ceases its steep decline only as the insolation drops to zero. From then on, the average air temperature is governed by the release of thermal energy stored in the environment over the day, and decreases at a slower rate throughout the night, until shortly after the insolation begins to rise in the morning. As one would expect, the relative humidity tracks the changes in the average temperature well, and falls as the spatial average temperature rises.

C. Correlation of the Diurnal Difference Pattern with Sensor Location

In this section we relate the morphology of each location to the features of its diurnal difference pattern. As we did not measure wind speed and direction or surface energy balances in the vicinity of our measurement locations, the association of microclimate effects with a given location are tentative. The assertion of relative strengths of similar microclimate effects, for example shade versus evapotranspiration are also hypothetical. Table 2 summarizes the behavior of the temperature difference, and lists the day an night- time microclimate effects that we expect to be active at each location.

1. Patterns of Type 1

Diurnal difference patterns of type 1 show a wide range of morphologies, some with single and other with double or even triple local maxima and significant dips between them (the basic pattern however is still "peak"). They also vary in the timing and width of the main extremum more than patterns of type 2. They come from a diverse set of locations, some quite near the house, and others further away than locations exhibiting patterns of type 2. But, none are under tree canopy. Some, like location 11, are near trees, but not under them or inside the foliage. At locations near the house and under or next to tree canopy, a competition can take place between the cooling effect of the tree and the warming effect of the house, leading to patterns of type 3.

a. Daytime

The hierarchy in the strength of the daytime microclimate effects seen in Figure 5a can be explained in terms of the site morphology. The difference patterns for locations 6, 10, and 11 show a large warming effect next to the house, or in close proximity (within 4.5m) on the south and east sides. Temperatures typically reach 1.5 to 2 °C warmer than the spatial average over the course of the day. On the other hand, sensors 9 and 18, placed at a somewhat larger distance from the south side of the house, show a daytime deviation in the range of 1 to 1.5 °C warmer than the average. The anomalous increase in temperature with height at this location may result from advection from the house: sensors 10 and 11 nearer the house show yet higher temperatures at 1.5m above the ground.

Sensors 1 and 16 show difference patterns which increase to slightly more than the spatial average during the first half of the day. However, the air temperature difference drops rapidly, to about 0.6 to 0.8 below the average, during the same hour that the average reaches its maximum. Sensor 1 is over a surface of moderate albedo (light colored gravel) about 5m from the west side of the house. While only slightly more distant from walls of the house than sensors 9 and 18, and on the same type of surface (sparse grass), location 16 is usually out of the wind shadow of the house during the day. In addition to being well separated or generally upwind (during daylit hours) from sensible heat producing features, the environments around 1 and 16 are the most open to the sky (excluding 17 on the roof).

The characteristic 1 p.m. drop in the difference patterns results from the fact that air temperatures in these locations reach a (smaller) maximum about 1/2 to 1 hour earlier than the spacial average. Until the early evening, the temperature profiles at 1 and 16 lead the spatial average by about the same amount, indicating less thermal storage in the local environments of these sensors relative to the others in the average. It could result from a local deficit in net incoming radiation, due to higher than average reflectivity, or a local excess of evaporation or ground flux.[4] It may also be that wind or advection factors could be larger in these open locations than elsewhere around site.

Patterns from locations 9, 18 and 11, on the east side of the house, show a small trough immediately preceding the peak, while sensors 1 and 6, on the west side of the house show a small trough immediately after. The timing results from the fact that the eastern locations are shaded for some interval after sunrise, and the western locations are shaded for some interval before sunset, by vegetation at the edge of the property. During these intervals, most of the other sensors are not shaded. Sensor 6 is also shaded by the large walnut tree during part of the late morning, and by the house itself over much of the afternoon.

It becomes more difficult to explain some of the finer details of the diurnal difference patterns based on temperature and insolation data alone. For example, the break in the rise at about noon for sensors 9 and 18 seems to occur most days of the run, but no cause was apparent.

---

[4] We cannot exclude evaporation from location 1, because we did not measure soil moisture under the gravel, and we cannot exclude cooling from high albedo surfaces at 16 because it is near the cement pool deck.

b. Night-time

While the daytime temperature difference mainly reflects the partition of net incoming radiation amongst sensible heat, evaporation and surface warming in the local environment, the night-time value is often an indication of the ability of local surfaces to radiate stored thermal energy at night. Sensors 1, 16, and 18 show temperatures well below the spatial average at night. The local environments of locations 1 and 16 are open to the sky (high view factors), and therefore capable of quickly cooling by long wave radiation at the end of the day. Neither location is typically in the wind shadow of the house. The profiles of sensor 9 and 18 may show the effect of the night-time temperature inversion over the ground surface, although it is difficult to explain a 1.3 °C difference over less than 1 meter in height by appealing only to this effect.

Although location 6 has a very low view factor, it is well shaded in the late afternoon, and well ventilated by air flow through the channel formed by the pool house and house walls. Air velocity is typically higher in this channel than around other sensor locations. Thus the ambient air temperature at location 6 is closer to the spatial average than other sensor locations near the house. Locations 10 and 11 have low view factors and are not well ventilated, as reflected in their higher night-time temperatures.

2. Patterns of Type 2

From Table 1 we see that, of the locations which show a daytime depression in their diurnal difference patterns, all but number 17 are under or near shade trees or other large vegetation. Lowered air temperatures in these locations can result from shading of local surfaces as well as from evapotranspiration during the day. Unlike those of type 1, we tend not to see the small dips associated with morning and evening shading of the sensor in type 2 patterns: if there, they are obscured by the main trough.

a. Daytime

Microclimate Effects near Trees

For type 1 patterns, we found a ranking based on the size of the of the daytime maxima in the difference patterns, which correlates roughly with the distance from and orientation relative to the house. A ranking of type 2 patterns which come from locations near shade trees can be made on the basis of the depth of the local temperature depression in Figure 5b. From greatest to least are: Sensor 5 in the canopy of the large walnut tree, where both shade and evapotranspiration reduce ambient air temperature; sensor 7 in the canopy of a much smaller Mulberry tree; and sensor 4, on the trunk, where the main effect is shade from the extensive foliage.

Location 7 takes longer to reach and spends less time near its minimum than any other location near trees. This may from competing microclimate effects; heating from the structures and cooling from the tree and shade. Comparing nearby sensor locations, we see that the coolest air relative to the average occurs at location 7 after 1 p.m., when the heating effect at location 6 has been reduced significantly.

14

The data are not inconsistent with the idea that, differences in water availability aside, the magnitude of the local temperature depression is positively correlated with the volume and density of the tree canopy, and is greatest in areas where shading and evaporative cooling effects are combined. We excluded location 19 from the ranking because the sensor was, technically, neither attached to the foliage or the trunk of a tree. Instead this sensor was placed about 1m from the nearest tree trunk in a numerous stand of redwoods, occupying the 1.2 m incline extending from neighboring property to the edge of the cement drive near the carport. Here, the cooling effect is as strong or stronger than that at location 5. There is also a great deal similarity between the diurnal difference patterns for sensors 4, 5, and 19. The redwoods shade the surface below them, which consists of moist soil covered with a mulch of dead needles and other debris at least 2 cm thick. Thus, it is likely again that both evaporation and shading effects contribute to the air temperature depression at location 19.

Evaporative Cooling and Shade

Sensor 8 is slightly further from the nearest trees or other tall, dense vegetation than the others which show a type 2 pattern, but the local environment may be shaded by redwoods in the creek banks to the south for a good portion of the day. When only diffuse radiation from the northern half of the sky is received, it is not unusual to find dramatically lower near-surface temperatures than at surrounding sunlit areas (Stoutjesdijk, 1980). Location 8 is also near the pool (not heated) and the creek banks. Air at this location may be cooled by evaporation at the surface of the pool, or advected from near the walnut trees or the creek. The later seems less likely when one considers the warmer air temperatures at sensor 2 and 4.

Trapped or Channeled Air In Shady Areas

The difference patterns of location 2 and 3 highlight the effect of height on air temperature over a shaded depression in the landscape. Open only to the north-west, and partially above, both locations receive about the same amount of shading. They show roughly similar patterns, with 3 offset by about -1°C from the other. Location 3 may be the recipient of cool air trapped or channeled along the creek bed. Shading from the south may also contribute to an increased share of long wave loses in the energy budget, resulting in the ground surface (and air at the lower height) being considerably cooler than the air above it (Stoutjesdijk, 1980).

Competition between Heating and Cooling Effects

On the other side of the house, locations 14 and 15 (in front of the house) may experience both heating effects from surfaces and cooling effects from local vegetation. These locations are in proximity to heat sources such as the roof, walls, and driveway. Wind speed is also reduced locally by the fig tree, and Camellia bush, and possibly the large redwood tree. It is not clear whether 15 merely shows the result of radiative trapping at night or if microclimate effects also play a role during the day. At 14, placed further from the drive and closer to large vegetation, walls and the roof, a cooling effect clearly dominates in the morning (likely shading of the local environment and some evapotranspiration), but heating effects take over by mid afternoon.

b. Night-time

The diurnal difference patterns for locations 5,7, 8, and 19, show that the temperatures in these locations are usually at or below the spatial average during the night. Away from the house, it seems that radiative trapping is not very effective in keeping night-time temperatures high when at least half the sky is visible (locations 8,19). While radiative trapping may be effective below the canopy of dense trees (location 4), interior and upper layers of the canopy (5 and 7) are screened from the long wave radiation emitted by the ground, so that successive layers in the canopy are cooler than the ones below (Terjung and O'Rourke, 1980).

Both locations 14 and 15 show significant elevations in the night-time temperature (0.6 and 1.3 °C respectively). There is significantly reduced sky view from the north wall of the house near location 15 and more so near 14. Thus, radiative trapping may be important near the house in the presence of large or dense vegetation. One might expect 14, with the denser vegetation, to have the higher night-time temperature. But sensor 14 is near a corner of the house which is partially shaded, and the adjacent wood fence has little thermal mass. In addition, sensor 15 is closer to the courtyard, the walls and paved walkways of which have low view factors.

c. Daytime Heating with a Night-time Inversion

Inspecting the pattern and not the values for sensor 17 (roof tower), one might hypothesize some type of cooling effect during the day. But location 17 is the only location showing type 2 behavior for which the ambient air temperature is always significantly higher than the average. Although it is the most open to the sky of any sensor location, 17 has the highest night-time temperature of any of the sensors[5]--typically about 2 °C higher--indicating that heating effects are dominant here both day and night. It may just be that the sources of warm air during the day and during the night are different, and yield two different values of the temperature difference.

Data from a thermocouple placed under a roof tile on the west side of the house for the first two weeks of the experiment shows that, while the roof temperature rises to over 40 °C on a typical day, the roof cools down rapidly at night, reaching to within a degree or two of the average air temperature at dawn.[6] It is indisputable that heating from the roof is a factor during the day, but is unlikely to be the cause of the high night-time value.

One possible explanation is that a thermal inversion sublayer builds over the site as the ground surface cools in the evening. Then location 17, about 4m higher than the others, would be warmer at night than locations with sensors used in the average. Inversion sublayers are known to form at ground level, less than 2 hours before sunset, and may build in height and strength over the night, only to disintegrate rapidly in the 1.5 hours after sunrise as the stratification is broken up by convection; these intervals being somewhat smaller for a height of 4 or 5m above the ground (Geiger, 1965). Such a time evolution is a good match to the diurnal difference

---

[5] We exclude sensor 13, because of its suspiciously large offset.

[6] We did not calibrate this thermocouple, but we assume that it is like the others, and calibration will change the temperature by no more than about ±2°C. Also, this temperature was known to change by several degrees depending on the position on the roof. Thus, the general nature of the statement about the temperature on the roof surface.

pattern for location 17. It is noteworthy that the heating effect of the roof at maximum gives a smaller air temperature elevation from the average than the night-time inversion.

3. Patterns of Type 3

While we have doubts about the calibration for sensor 13 (east cherry tree), errors in calibration are not expected to change the gross shape of the difference pattern, because calibration is a linear transformation of the data. So, we expect the difference pattern for location 13 to be of the shape shown, but probably shifted down by at least 1°C.

The pattern is unusual in that it is the only one of type 3, showing a large amplitude trough followed by a large peak during daylight hours. In the difference pattern, we see the competition between the heating and cooling effects during the day. After sunrise, large trees to the east shade the cherry tree in which the sensor hangs; the north wall of the house west of the tree and the ground below it remain shaded. The difference pattern following sunrise is like any other in the canopy of a tree (5 and 7). As the sun rises, the roof, east wall and ground receive an increasing flux of short wave radiation. By 9 a.m., the rate of heating from these sources overtakes the rate the cooling from the tree or north wall. By mid-morning, the heating contribution has clearly squelched any cooling signal, and around noon the temperature difference has reached a maximum, about 1.2°C warmer than the morning minimum.

There are similarities between the patterns for 11 and 13 during the day, the morning troughs being 0.4 and 0.7°C deep, respectively. While 11 is shaded slightly longer than 13 in the morning by the eastern trees, it is not in tree canopy like 13, but several meters between canopies of small trees. Thus the smaller morning trough.

We do not attempt to examine in detail the night-time behavior of this sensor without knowing the offset of the pattern from where it should be. It is, however, likely that night-time temperatures are influenced by radiative trapping, similar to location 15. The canopy is somewhat denser and closer to the eaves and wall at 13 that 15, and the east walls receive more direct sunlight than the north ones. Other factors excluded, we would expect a larger night-time temperature difference at 13 than 15.

Clearly we have seen, at least for this experiment site, that there is a strong connection between the diurnal patterns of each sensor and the microclimate effects that can be inferred from the local environment of each sensor, satisfying the second hypothesis of this experiment.

D. Bias in the Spatial Average

1. Bias from Choice of Sensors

Of the 13 sensor locations used in creating the spatial average, we find from the above analysis that 7 of these locations show diurnal difference patterns of type 1 (locations 1,6,16,9,18,10, 11), and 6 show patterns of type 2 (3,4,5, 7,15, 19). Inclusion or exclusion of one or two sensors in the average does not change the basic classification of these diurnal patterns. So, at least, we have not overly biased the average by inclusion of too many data sets of one type, there being

roughly equal numbers of both types in the average.

Because of their separation from and orientation relative to microclimate producing features of the site, one could expect locations 1 and 16 to be less affected by local microclimate effects than most other sensor locations during the day. Indeed, air temperatures at these locations do not depart significantly from the spatial average during the period 8 a.m. to 1 p.m. This can be taken as an indication that the bias of the spatial average introduced by the choice of particular sensors included is not very significant, at least during this interval. But after 1 p.m., air at 1 and 16 is on the order of 0.5°C cooler than the spatial average. What this means in terms of bias is dependent on the meaning attached to the spatial average. If the spatial average is to represent the temperature of air unperturbed by localized heating and cooling effects, as it advects onto the experiment site, then it may be biased on the warm side by the fact that seven of the other sensors in the average are in close proximity to the house, mainly on the south and east.[7] It is possible then, that the effect of radiative trapping is more extensive than shown by the diurnal difference profiles of the last section.

But if the spatial average is considered to be, as its name suggests, the mean temperature at 1.5 meters of air flowing over the entire site, then the afternoon T_{ave} simply shows the effect of thermal storage on air temperature at the experiment site; because the division of sensors in the average is roughly even amongst the two types, the bias of our computed average is probably smaller than 0.5°C in the afternoon.

2. Bias from Misidentification of Sensors

Not shown in Figure 3 is a discontinuity in the data and patterns for sensors 9 and 16 on October 6 (Julian day 279). Records of the experiment indicate that modifications were made to some of the connections to the data logger on that afternoon but not those for sensors 9 or 16. Because of an ID check of each connection to the logger performed at the post-calibration, we are certain to which channel each sensor was connected at the end of the data run. As there were no discontinuities in these signals after October 6, we can be certain that sensors 9 and 16 were connected to these same channels from then on, but we are not certain of the origin of these signals prior to this time.

Clearly, if the average is only to contain data from sensors which do not fail or change identity during the data run, it is necessary to exclude sensors 9 and 16 from the average over the entire run, or not use the spatial average before October 7. The spatial average was computed early in the data reduction, and used extensively before the problem was discovered, so we chose the later. The preceding analysis was based on Julian days 285 through 299, and is not affected.

---

[7] It is difficult to explain the rapid drop in the patterns for 1 and 16 to -0.6 and -0.8 °C below the average after 1 p.m. as a genuine cooling effect (Figure 6). These locations should reflect the temperature of air moving through the property, only mildly perturbed by local microclimate effects.

E. Microclimate Effects and Maximum Daily Temperature

1. Choice of Synoptic Variables

So far we have concentrated on the identification of the microclimate effects through the diurnal difference patterns and the morphology of the measurement locations. While the shape of the patterns remain largely the same over the course of the data run, the daily minima or maxima, for example, vary from day to day. For each sensor location we now examine the variation in these extrema as a function of site temperature over the course of the data run.

To simplify the analysis, we use synoptic variables--one parameter which summarizes the difference profile, and one parameter which summarizes the spatial average of the ambient air temperature, for each day of the run.[8] For the spatial average we choose the daily maximum, which will allow us to compare "hot" and "cool" days in a systematic way. But we are still free to choose amongst a variety of possible parameters to represent the microclimate effects for each day. Here we use the daytime extrema of the subtractions, i.e. the value of the greatest local maximum for difference patterns of type 1, and the least local minimum for the type 2. As previously indicated, these values do not necessarily represent the largest absolute temperature difference from the spatial average, i.e., the maximum net microclimate effect for the day. Instead, the daytime extrema reflect the influence of the most dominant microclimate effects near the middle of the day.

To gain a feel for the conditions at the site over the interval used in the regressions, we show histograms of synoptic climate variables in Figure 7. We did not have cloud or rain detectors at the site, nor was any record kept of these events by the occupants of the house. A day for which the maximum insolation is relatively low indicates clouds over the site, while a maximum relative humidity measurement above 95% generally indicates rain.

While it is not possible to predict the local temperature variation near any assortment of shade trees and residences from such a limited experiment, our results do give an indication of how much local variation in temperature correlates with the overall site temperature. Recall that we are not asserting a causal relationship between average air temperature and the strength of local microclimate effects, but rather searching for a useful indicator of how strong one might expect these effects to be on a given day.

---

[8] Using difference data for more than one time in the day combines the response of microclimate effects with different origins, and different timing, to changes in the average temperature, thus producing too much scatter to make the regressions meaningful. Another way of seeing this is to note that the timing difference between the spacial average and the difference plots leads to a double valued temperature difference for each value of the average temperature for each day; additional scatter results from the fact that the same average temperature may occur at different times on different days, under quite different conditions (and microclimate effects). Thus, the results of such regressions are usually inconclusive.

2. Exclusion of Data Points

For most sensor locations, the interval from which the data was taken is the entire interval over which the average is good (Julian days 280 through 322, inclusive). The gap in the interval for sensor 14 covers the time the sensor was briefly plugged into a channel in which it was not calibrated. The early termination of the interval for sensor 15 results from the fact that the diurnal pattern had changed to such an extent as to make the minimum something other than what it means in the context of Figure 5. This was the only diurnal pattern that changed appreciably over the course of the run.

We also eliminated certain days within the interval over which the regression was performed. The daily extrema were found by computer program, so we eliminated any day for which we could not guarantee the result was real and not caused by instrument error. We also exclude data from day 279, as interruption of the data run lasted most of the day.

In the process of performing the regressions, we found a handful of problematic data points which were extreme outliers, generally more than 1°C from the regression line. Most of these came from days in which the extremum came more than several hours away from the expected range of times encountered in the data set for that sensor. We therefor excluded days in which the extremum occurred outside the period 7 a.m. to 5 p.m., or about 1/2 hour after sunrise to about 1/2 hour before sunset.[9] Thus, anomalous timing and instrument error were the only cases requiring elimination of points from the interval of regression.

3. Results of Regressions

Table 3 shows the results of regressing the daytime extrema of the subtraction for each sensor location against the daily maximum spatial average temperature. The daytime maximum was used in the regressions for sensor locations yielding patterns of type 1, and the daytime minimum was used for patterns of type 2. A horizontal bar separates the two. The results of the regressions are shown in the last four columns of the table. The intercept is calculated for a day with a maximum spatial average temperature of 25 °C. That is, the equation for the regression is

$$\Delta T_i^{ext} = m(T_{ave}^{max} - 25) + b,$$

where "ext" means the daytime extremal value. The final column is the probability that these trends could be found in a subset of a parent population which showed a slope of 0 or of the opposite sign as that in Table 3 (calculated from the student t-statistic).

The most striking feature of the table is that, except for sensor 17, the regressions yield positive slopes for the patterns of type 1, and negative slopes for the patterns of type 2: the slope and the intercept are always of the same sign. This result indicates that the dominant microclimate effect at the time of maximum grows *stronger* with increasing temperature. In the case of location 17, we see from the large offset of the diurnal difference pattern that the dominant effect at

---

[9] Nine of the 16 days excluded from the interval for sensor 15 could also be excluded on this criterion.

20

all times is heating from the roof. We should not be surprised, then, to see that the slope for this sensor is positive, as the daytime heating effect responsible for the minimum is generally stronger on warm days than on cool ones. Similarly, some confidence that cooling effects are active at location 15 during the day is had by noting that the temperature difference is generally more negative on warmer days.

From the intercepts, a ranking of the microclimate effects for the locations near trees emerges, which, as one would expect, reproduces that found from Figure 5 (see Section V.C.2.).

All of the slopes found in the regressions are significant at the 99% level, except that for sensor 6, which is not even significant to 90%. In this simple bivariate model, we see that the temperature difference is expected to grow typically by a few tenths of a degree for each 10 degree change in the daily maximum average temperature. Yet, the squares of the correlation coefficients demonstrate that typically only about 45% of the variance in each data set can be explained by this model.[10]

4. Time Slice Regression of the Difference with the Spatial Average

Our method in the last section, i.e. correlating events that may occur hours apart, and in any temporal order, was only meant to establish a trend of microclimate effects with average temperature. To satisfy any remaining objections to the method, we repeat the process with variables measured simultaneously. Table 4 shows the results of regressing the temperature difference against the spatial average temperature, both measured at the maximum of the later. This time is generally different from day to day, but generally between the hours of noon and 3 p.m.

As the sampling occurs generally at some time other than when the temperature difference reaches an extremum, we expect the slopes and intercepts of these regressions to be less dramatic than those of Table 3. The regressions for locations 1, 6 14, 15, and 16 even show a slope or intercept of the opposite sign. These (except location 6) show a diurnal difference pattern in the process of making a rapid transition at the time the average temperature pattern reaches its maximum; on a day to day basis, the sampling occurs at some random point in the transition, yielding essentially a random value in the interval between the daytime extremum and the night- time value. Thus, these regressions have a higher probability than the others in Table 4 (or any in Table 3) that the trend found is not significant. On the other hand, the difference at location 6 typically has completed its decent to its shaded, afternoon value, and shows a stronger correlation with the spatial average temperature than in Table 3.

Regressions for the other sensors show the same trends as Table 3, but often with smaller slopes, intercepts (in absolute value), and correlation coefficients. However, the significance of the slope is not notably affected for these, as the number of points is large. The conclusion of the last section is only slightly modified: unless there is a transition between two competing microclimate effects at the time, the dominant microclimate effects at the time of maximum temperature tend to be stronger on hot days than on cooler ones.

---

[10] The R^2 can be computed as the model variance over the sample variance (see for example Hamilton, 1992).

F. Locations Exhibiting Minimal Microclimate Effects

The local ambient air temperature at the location of sensors 1 and 16 generally do reflect the average to within one half degree, for ambient air temperatures less than 25 °C, over the period 8:30 a.m. to 1:00 p.m. These are locations generally out of the immediate wind shadow of the structures during the day, with the highest view factors and the largest distance from trees or man made objects (excluding the pool) of all the sensors.

Yet, our analysis shows that it is likely than none of the sensor locations in this experiment show *negligible* microclimate effects over all daylight hours. If the lot were proportionately larger, we believe that moving the sensor locations radially away from the house would reduce the influence of heating effects on the measurements. But our results indicate that lots with this type and density of land use may not be suitable at all for measurement of neighborhood temperatures, much less their comparison, at 1.5 meters; microclimate effects are nearly *everywhere* this close to the ground, and any neighborhood scale signals related to albedo or vegetation are likely to be swamped by systematic effects.

G. Locations for Measurement of Neighborhood Temperature

The large differences in air temperature found at locations in close proximity indicates that the "footprint", or area which contributes most significantly to the microclimate effects, for a point 1.5m or less over the ground surface, is exceedingly small--generally less than 5m in radius at our site in Lafayette. Yet, in some previous studies, measurements at about this height in dense suburban locations have been interpreted as representative of a neighborhoods up to 104m2 (Sailor et al, 1993; McGinn, 1982), when they are probably much more location specific.

The influence of local microclimate effects on neighborhood temperature measurement could likely be reduced at a site with more open space, less densely packed structures, and which is outside the canopy layer of local windbreaks. But these requirements can conflict with the range of vegetative density or albedo necessary to conduct an indirect effect experiment, or may overly limit the choice of siting in urban or suburban areas.

The only alternative seems to be to raise the sensors to a height negligibly influenced by any particular element in the immediate environment. Indeed, most protocols for sensor siting seek to minimize microclimate effects by requiring sensors to be placed on towers, a minimum distance (generally 9 or 10 times height) from objects which potentially alter the local microclimate (EPA 1987, 1989). Temperature differences near the ground--at chest or structure height--between neighborhoods are not measured in this case, and must be calculated. A good sensor siting protocol for this purpose would incorporate a balance between the systematic errors encountered from microclimate effects and from vertical extrapolation of temperatures.

VI. Conclusion

The temperature data from locations around a suburban structure were analyzed to detect the presence of microclimate effects using a subtraction method with respect to a spatial average temperature constructed from the same data. The temperature difference from the spatial average formed a diurnal pattern unique to each sensor location, and the patterns for each of the

sensors could be classified into one of three types: those showing a significant daytime peak, a significant daytime trough, or both a significant trough and peak. The pattern type for each location correlates well with the attributes of the location. Locations near the house exhibit the first pattern; those near shade trees and other large vegetation with much foliage show the second pattern. Locations near the house and shade trees may exhibit the third pattern, reflecting a competition between heating and cooling effects. The night-time value of the pattern is generally correlated with the fraction of sky visible from surfaces around the location, indicative of the ability of the surroundings to cool at night.

Locations in relatively open areas, away from the wind shadow of structures or other objects, show a daily pattern of the first type, in which the temperature difference during the peak is the closest to zero, indicating the least amount of local microclimate effects. But, none of the measurement locations showed negligible microclimate variations over all daylight hours, illustrating the difficulty in finding locations to measure an unperturbed neighborhood temperature at 1.5m above the ground.

The microclimate effects operating during daylight hours correlate well with the maximum daily air temperature as determined from the spatial average. The influence of the dominant daytime microclimate effect strengthens with increasing temperature. Those patterns which show a dominant cooling effect during the day are negatively correlated with the maximum temperature, while those with a dominant heating effect are positively correlated with the maximum temperature.

Our experiment represents the first step toward quantifying the influence of microclimate variations in the suburban environment. Clearly there is a need for this information among groups as diverse as building energy modelers, urban climate researchers, and landscape architects. Future efforts should include measurements of a representative wind speed and direction over the site, and preferably at the location of several or all of the climate sensors. Detailed measurements of the energy balance at surfaces in the local environment of sensors can also help to discriminate between several potential microclimate effects near the measurement points.

ACKNOWLEDGMENTS

REFERENCES

Akbari, H., D. Kurn, H. Taha, S. Bretz, and J. Hanford. 1995. "Peak Power and Cooling Energy Savings of Shade Trees," Accepted in *Energy and Buildings - Special Issue on Urban Heat Islands*. Excerpts from Lawrence Berkeley National Laboratory Report LBL-34411,

Berkeley, CA.

Akbari H., S. Bretz, J. Hanford, D. Kurn, B. Fishman, and H. Taha. 1993. "Monitoring Peak Power and Cooling Energy Savings of Shade Trees and White Surfaces in the Sacramento Municipal Utility District (SMUD) Service Area: Data Analysis, Simulations, and Results," Lawrence Berkeley National Laboratory Report LBL-34411, Berkeley, CA.

Akbari, H., A. Rosenfeld, and H. Taha. 1990. "Summer Heat Islands, Urban Trees, and White Surfaces," *Proceedings of American Society of Heating, Refrigeration, and Air Conditioning Engineers*, Atlanta, GA, (February). Also Lawrence Berkeley National Laboratory Report LBL-28308, Berkeley, CA.

Atwater, M.A. 1972, "Thermal Effects of Urbanization and Industrialization in the Boundary Layer: A Numerical Study", Boundary Layer Meteorology, 3, pp. 229-245.

EPA, 1987, "On-Site Meteorological Program Guidance for Regulatory Modeling Applications, Office of Air and Radiation, EPA-450/4-87-013.

EPA, 1989, "Quality Assurance Handbook for Air Pollution Measurement Systems", Office of Research and Development, Atmospheric Research and Exposure Laboratory, EPA-600/4-90-003.

Geiger, R. 1965, The Climate Near the Ground, Harvard University Press, Cambridge.

Hamilton, L.C., 1992, *Regression with Graphics: A Second Course in Applied Statistics*, Brooks/Cole Publishing, Pacific Grove.

Heisler, M., S. Grimmond, R.H. Grant, C. Souch, 1994, "Investigation of the Influence of Chicago's Urban Forest on Wind and Air Temperature within Residential Neighborhoods", in "Chicago's Urban Forest Ecosystem: Results of the Chicago Urban Forest Climate Project", McPherson, Nowak, and Rowntree, eds., Gen. Tech. Rep. Ne-186, USDA, Forest Service.

Huang, J., H. Akbari, H. Taha, and A. Rosenfeld. 1987, "The Potential of Vegetation in Reducing Summer Cooling Load in Residential Buildings," *J. of Climate and Applied Meteorology*, **26**(9), pp. 1103-1116. Also Lawrence Berkeley National Laboratory Report LBL-21291, Berkeley, CA., July 1986.

Jensen, M.E., and H.R. Haise, 1963, "Estimating evapotranspiration from solar radiation", J. Irrigation and Drainage Division, Proc. Amer. Soc. Civ. Eng., **89**(IR4), 15-41.

Kurn, D. M., S. Bretz, B. Huang, and H. Akbari. 1994. "The Potential for Reducing Urban Air Temperatures and Energy Consumption Through Vegetative Cooling," *Proceedings of the ACEEE 1994 Summer Study on Energy Efficiency in Buildings*, Vol. 9, p. 155, Pacific Grove, CA, August 1994. Also Lawrence Berkeley National Laboratory Report LBL-35320, Berkeley, CA.

McGinn, C., 1982, Microclimate and Energy Use in Suburban Tree Canopies, Ph.D. Dissertation, U. of Cal. Davis.

Oke, T.R., 1978, *Boundary Layer Climates*, Methuen & Co., London.

Sailor D., H. Akbari, and L. Rainer, 1992, "Measured Impact of Neighborhood Tree Cover on Microclimate," *Proceedings of the ACEEE 1992 Summer Study on Energy Efficiency in*

Buildings, Vol. 9, p. 149, Pacific Grove, CA, August 1992. Also Lawrence Berkeley National Laboratory Report LBL-32419, Berkeley, CA.

Stoutjesdijk, P., 1980, "The Range of Meteorological Diversity in the Biological Environment", Intl. J. Biometeor., **24**(3), 211-215.

Taha, H., H. Akbari, A. Rosenfeld, and J. Huang, 1988, "Residential Cooling Loads and the Urban Heat Island--The Effects of Albedo", Building and Environment, **23**, 271-283.

Terjung, W.H. and P.A. O'Rourke, 1980, "An Economical Canopy Model for Use in Urban Climatology", Intl. J. Biometeor., **24**(4), 281-291.

Sensor	Name of Location	Sensor Height (approx.)	Description of Location	Nearby Objects (horizontal distance)
1	West Patio	1.5m above ground	Open gravel area to west of house	1m tall wood and wire fence (4m) Eaves of House (4.5m)
2	West Bridge	0.8m above bridge floor 6m above creek bed	On partially shaded bridge over dry creek, at about ground level for the surroundings	Redwoods in south stream bank (7 m) Walnut trees on east bank (4 m)
3	West Under Bridge	1.5m above soil on slope 2.5m above bottom of creek bed	Under bridge, directly below sensor 2	Same as 2
4	South Tree (Trunk)	1.5m above patio 3m above dirt	Trunk of large English walnut tree about 2m up	Pool house (4m) Cement patio (.7m)
5	South Tree Canopy	2m above patio 3m up tree	Lower canopy of same tree as (4)	Pool House (5m) Patio (over)
6	South West Eaves	2.5m above walk	Below and adjacent to a section of roof connecting the main house to the pool house	Roof of house (0.5m) Pool house (0.6m) Cement patio
7	South Patio	2.5m above patio 2m up tree	Lower canopy of a small, sparse tree set in raised planter	Eaves of roof (4.5m) Patio (0.5m)
8	South Pool	1.5m above ground	In evergreen bushes adjacent to south side of pool	Pool deck (1m); Pool (4m) Redwoods in stream bank (6m)
16	South Yard Near Pool	1.5m above soil	Near edge of yard adjacent to pool decking	Pool Deck (4.5m); Pool (8m) Edge of roof (10m)
9	South Yard High	1.5m above ground	Near center of lawn area adjacent to pool	Porch roof (9m)
18	South Yard Low	.7m above ground	On same pole as sensor 9	same as 9
10	South Yard Near House	1.5m above ground	Edge of backyard adjacent to house	Bedroom porch (0.5m)
11	South East Near Trees	1.5m above ground	In between peach and cherry tree, about 2m from edge of eaves of house.	Peach tree (3.5m) Cherry Tree (4m) Roof over porch (4.5m)
13	East Tree	1.7m above ground	In lower branches of densely foliated cherry tree	Roof over porch (1m)
14	North East Tree	1.5m above ground	Camellia bushes at N.E. Corner of house	Eaves of roof (1m) Large redwood trees (3m) 6' wood fence (2m)
15	North East Drive	1.5m above ground	Edge of very faded (oxidized) driveway	Small fig tree (1m from foliage) Edge of eaves (2.5m)
19	West Tree	2m above driveway 1.5m above soil under redwoods	Edge of drive, near stand of tall redwoods.	Roof of carport (2m) Tall redwoods (0.5m from nearest trunk but directly below canopy)
17	Roof Tower	2.5m above roof apex	On roof near chimney #1	West chimney (0.5m)

Table 1: Location and environment of the temperature sensors. Sensor are listed counterclockwise around the property. Heights above are accurate to better than 0.2m (heights less than 1.0m to better than 0.1m), horizontal distances to 0.5m (distances less than 1m to better than 0.2m).

Sensor Location	Diurnal Pattern Type	Potential Microclimate Effects		
		Day (ems=early morning shade, las=late afternoon shade)	Night view factor	Night other effects
1	1	morning: minimal obstruction to wind flow, minimal heating from ground; las	high	minimal obstruction to air flow, lack of stored heat in substrate
2	2	mostly shaded, some evapotranspiration, channeled cool air	low	height relative to sensor 3 in inversion sublayer over creek bed.
3	2	mostly shaded, trapped or channeled cool air	low	
4	2	shade at all times, evapotranspiration	very low	heating from patio
5	2	shaded at all times, evapotranspiration	very low	shielding by foliage
6	1	morning: heating from walls of house afternoon: shade from structure, wind corridor	low	high velocity wind corridor
7	2	day: shade, evapotranspiration, heating from walls afternoon: shade, evapotranspiration, wind corridor	reduced	shielding of foliage, possibly wind corridor air
8	2	morning shade, evaporation from pool, evapotranspiration of creek bank vegetation	reduced	
9	1	ems, possible heating from house walls or advection of heated air	high	
10	1	heating from walls and porch area	low	near porch area with very low view factor
11	1	morning: partial shade late afternoon: heating from structure;	reduced	heating porch area
13	3	ems, evapotranspiration afternoon: heating from walls	low	heating from porch area/corner of house walls (low view factor)
14	2	morning: shade; evapotranspiration late afternoon: heating from structure; evapotransp.	low	heating from structure walls
15	2	partial shade (afternoon)	reduced	heating from house wall (low view factor)
16	1	far from structure, usually out of its wind shadow	high	minimal obstruction to air flow
17	2	heating from roof	large	height above other sensors in inversion sublayer
18	1	ems, heat from structure, ground, less height from ground than 9	high	height below other sensors in inversion sublayer
19	2	ems,laf, total shade interior to stand evapotranspiration; damp substrate	reduced (v. low in stand)	lack of stored heat in damp substrate

Table 2: Potential microclimate effects at the locations of the sensors. For diurnal pattern type: 1 = significant daytime peak, 2 = significant daytime trough, 3 = significant daytime peak and trough.

Sensor	Interval(Jd)	Days Excluded	N	Slope	Intercept at $T_{ave}=25°C$	R^2	P(slope=0 or opp. sign)
2	280-322	11	32	-0.051	-0.44	0.394	0.000
3	280-318	0	43	-0.111	-1.85	0.547	0.000
4	280-322	0	43	-0.036	-0.71	0.384	0.000
5	280-322	0	43	-0.052	-1.51	0.558	0.000
7	280-322	0	43	-0.056	-1.29	0.682	0.000
8	280-322	10	33	-0.032	-1.42	0.215	0.003
14	285-322	7	31	-0.031	-0.80	0.487	0.000
14b	285-322	4	34	-0.031	0.05	0.348	0.000
15	280-306	0	27	-0.079	-0.49	0.352	0.001
17b	280-322	10	33	0.023	0.48	0.165	0.009
19	280-322	4	39	-0.041	-1.60	0.186	0.003
1	280-322	9	34	0.036	0.43	0.551	0.000
6	280-322	6	37	0.023	2.09	0.035	0.133
9	280-322	11	32	0.072	1.66	0.748	0.000
18	280-322	4	39	0.106	1.10	0.755	0.000
10	280-322	5	38	0.087	2.43	0.454	0.000
11	280-322	7	36	0.060	2.06	0.445	0.000
16	280-322	4	39	0.050	0.48	0.572	0.000

Table 3: **Regression of the daytime extremum of ΔT_i against the daily maximum of T_{ave}.** (Bar separates type 2 minima and type 1 maxima). All type 2 locations except 17, show a cooling effect relative to T_{ave} at 25°C. Except for 17, the slopes are negative, indicating that the local cooling effect at these locations grows with increasing temperature. All type 1 locations show a heating effect relative to T_{ave} at 25°C, indicating that the local heating effect grows with increasing average temperature. Although location 17 exhibits a daytime trough in its diurnal difference profile, it shows a small heating effect during the day, which generally grows with increasing temperature.

Sensor	Interval (Jd)	Days Excluded	N	Slope	Intercept at $T_{ave}=25°C$	R^2	P(slope=0 or opp. sign)
2	280-322	11	32	-0.041	-0.02	0.272	0.002
3	280-318	0	43	-0.067	-0.96	0.529	0.000
4	280-322	1	42	-0.041	-0.54	0.408	0.000
5	280-322	1	42	-0.048	-1.30	0.447	0.000
7	280-322	2	41	-0.061	-1.05	0.587	0.000
8	280-322	11	32	-0.031	-1.11	0.175	0.009
14	285-322	7	31	-0.021	0.32	0.026	0.195
14b	285-322	5	33	0.044	1.71	0.135	0.019
15	280-306	0	27	-0.030	0.43	0.021	0.220
17b	280-322	10	33	0.033	1.06	0.128	0.022
19	280-322	4	39	-0.043	-1.09	0.181	0.003
1	280-322	9	34	-0.016	-0.56	0.034	0.150
6	280-322	6	37	-0.032	-0.26	0.118	0.019
9	280-322	11	32	0.067	1.34	0.410	0.000
18	280-322	4	39	0.080	0.60	0.495	0.000
10	280-322	6	37	0.094	1.99	0.575	0.000
11	280-322	7	36	0.066	1.76	0.481	0.000
16	280-322	4	39	0.048	-0.40	0.283	0.000

Table 4: **Regression of ΔT_i against T_{ave}, both at the time of maximum T_{ave}.** Since the ΔT_i 's are not generally at their extremal values, the cooling or heating effects at 25°C are generally less and the slopes less dramatic than in Table 3. Some slopes and intercepts are even of the other sign (1,6,14,15,16), but significance of the fit is generally less for these. These show diurnal patterns in the process of making or having completed a rapid transition toward the night-time value at the sampling time.
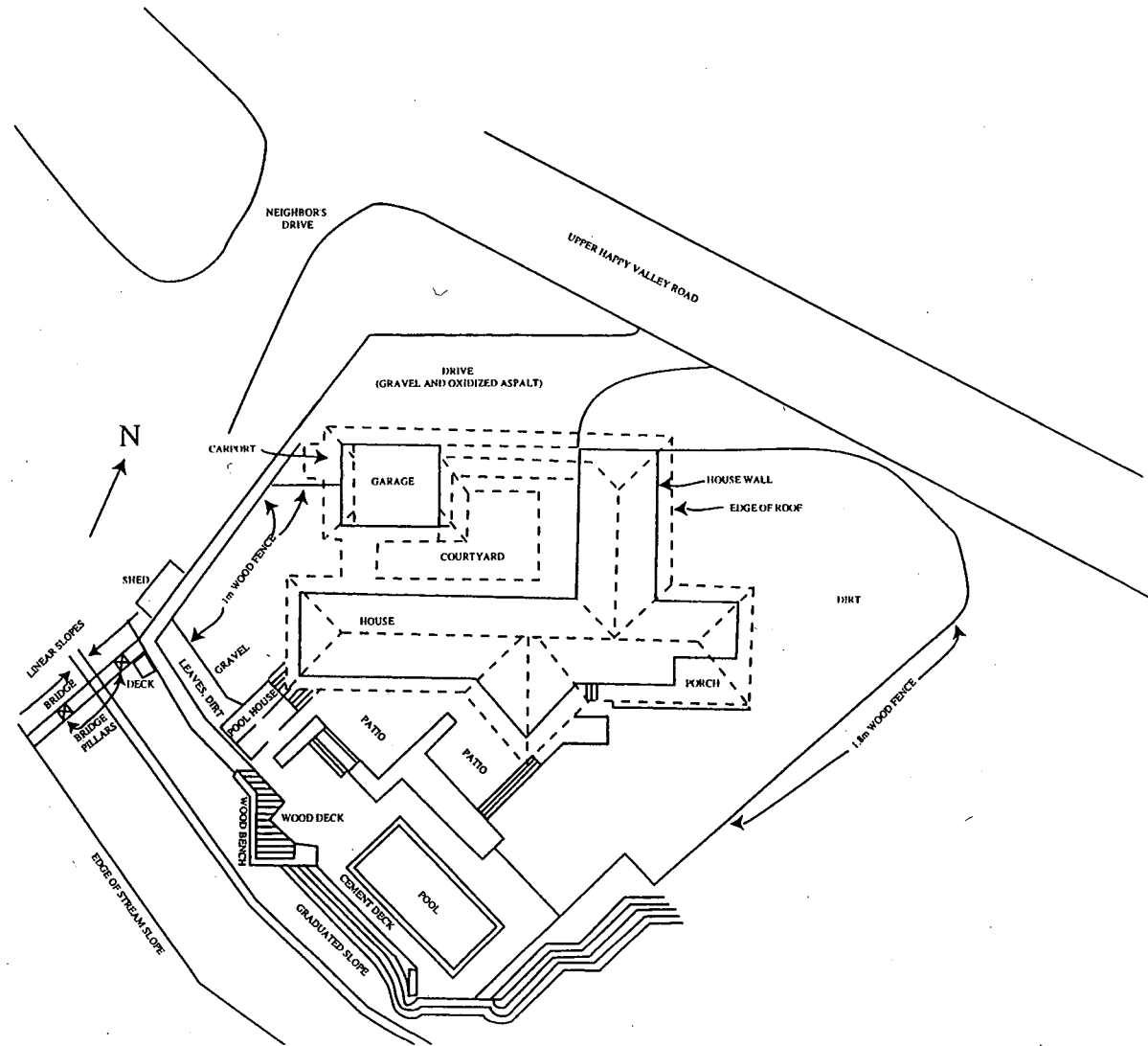
Figure 1a. The experiment site: outline of the structural and (non-vegetative) landscape features. Blueprints of the house and rear grounds were traced and scaled, while the eastern most area ("east grove") was drawn by hand to create this schematic. Walls of the house are shown as solid lines, and outline of the roof edge is dashed. Wood deck is shown as enclosed hatched area. Approximate scale 1cm ≈ 10m.
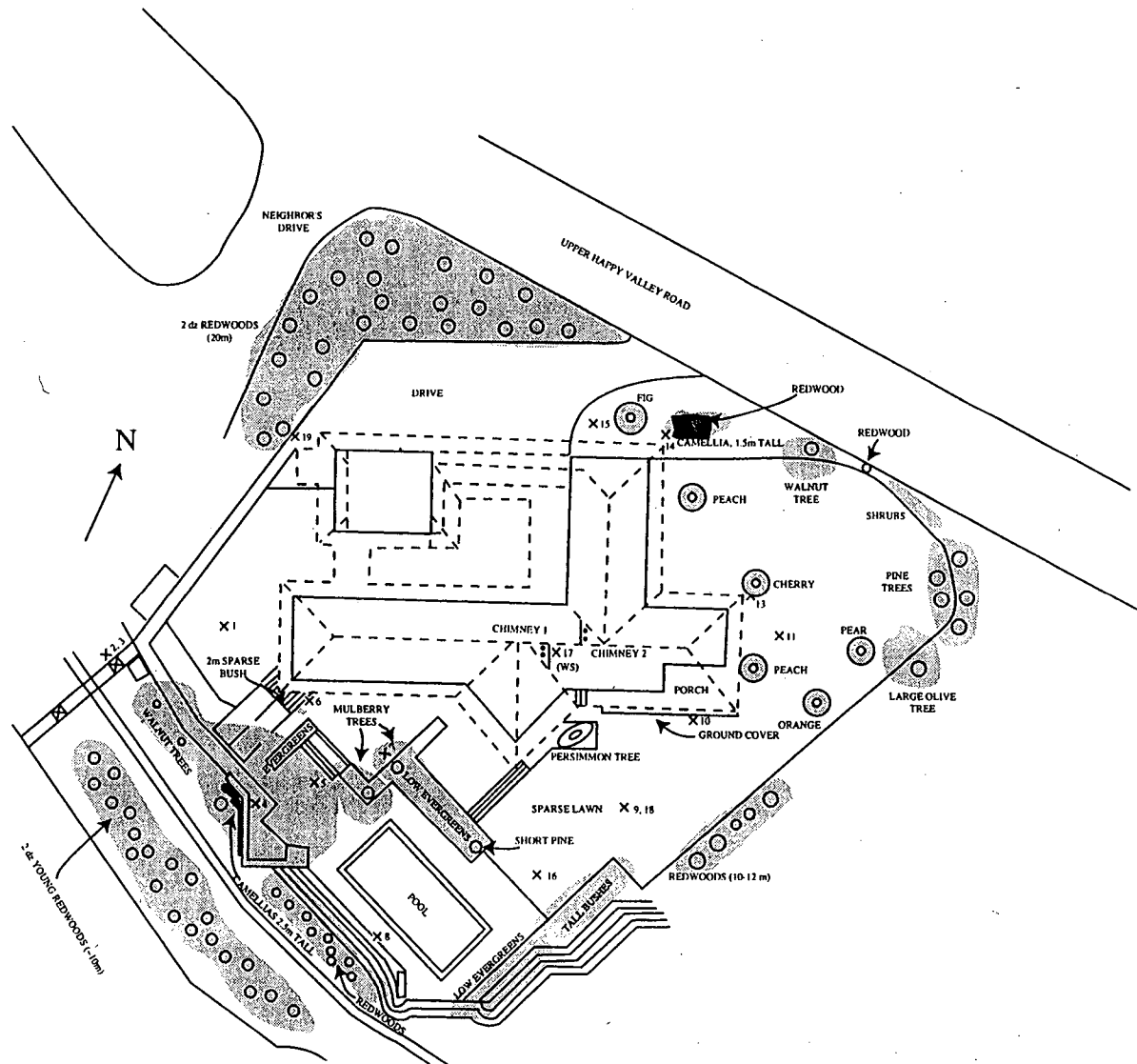
Figure 1b. The experiment site: location of temperature sensors, weather station, and vegetation. Individual trees are shown as a circle, representing the location of the trunk, and a shaded area indicating the extent of the canopy. Well manicured fruit trees are shown as two shaded concentric circles or ellipses. Large patches of shading indicate more or less continuous canopy. Large Camellia bushes under redwood canopy are more darkly shaded. X=Sensor location (numbered); WS=weather station.

Thermocouple
wire

.5" thick black armaflex insulation

Aluminum tape

Junction

.75" ID
white PVC pipe

Screen

Air intake

Fan
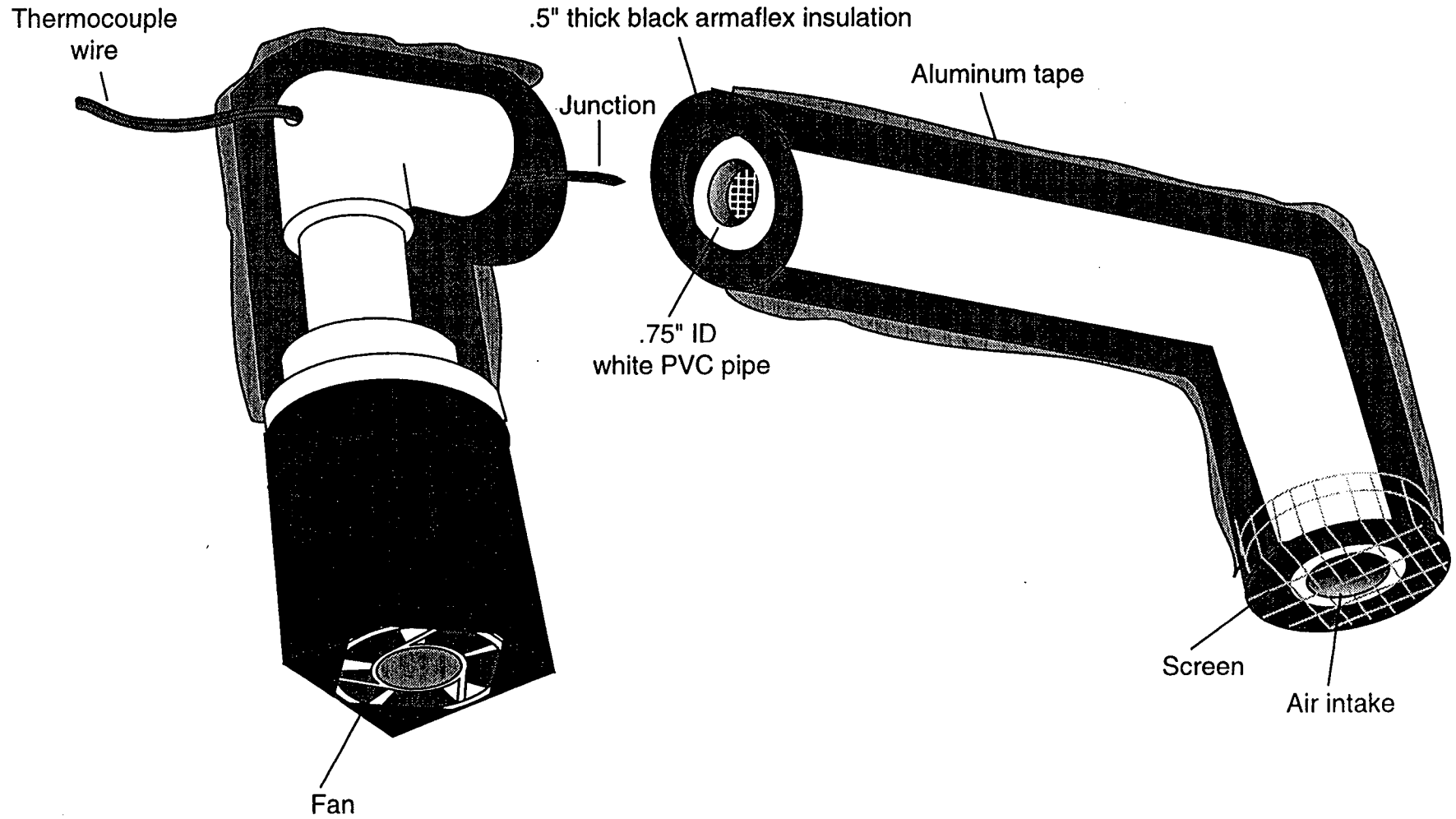
Figure 2. Construction of a temperature sensor. Air is drawn from right to left. The screen over the air intake is actually much smaller mesh than shown.

Insolation

Relative Humidity

West Patio (1)

South Tree Canopy (5)

South Yard High (9)

South East Near Trees (11)

Tower on Roof (17b)
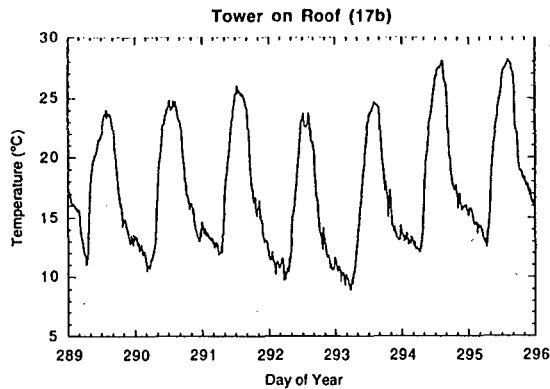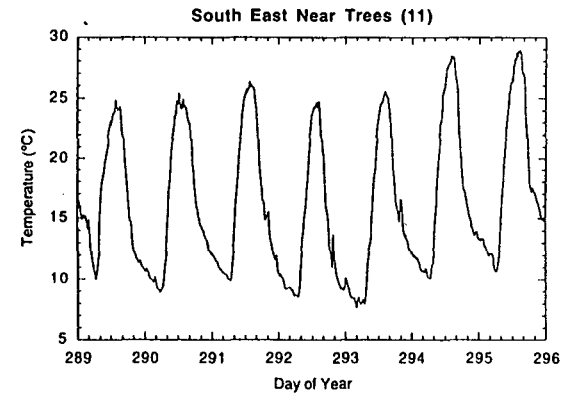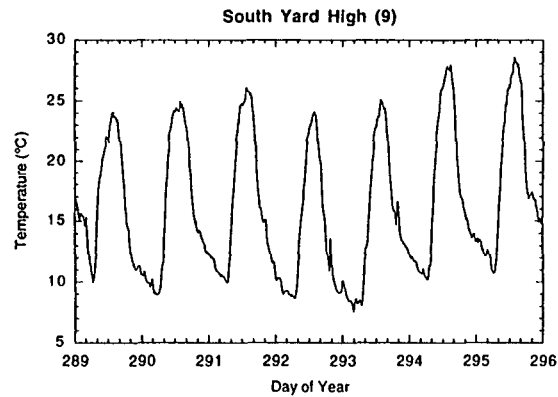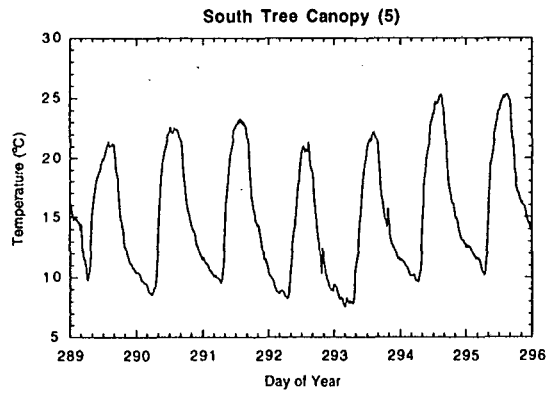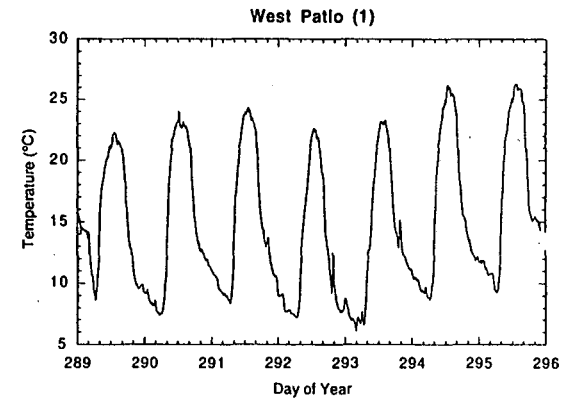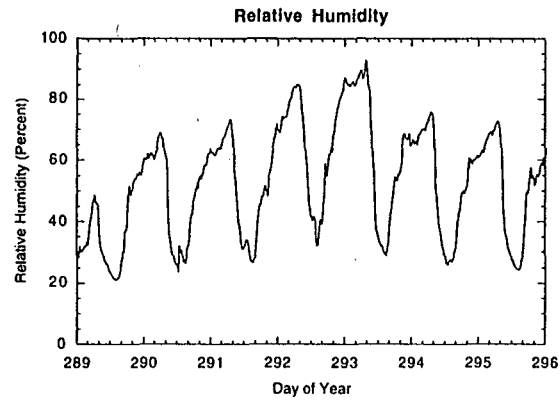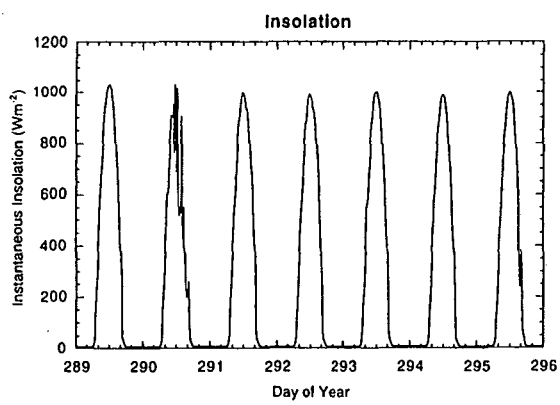
Figure 3. Calibrated data for selected sensors. The sensors were selected to span the types of behaviors that will be shown later (Figure 5). The time interval was chosen to exclude interruptions in the data acquisition for these sensors. At this stage, the only differences between the temperature plots that are obvious are gross features such as the values of daily extrema. Daily maxima of the insolation are good to ±5%.
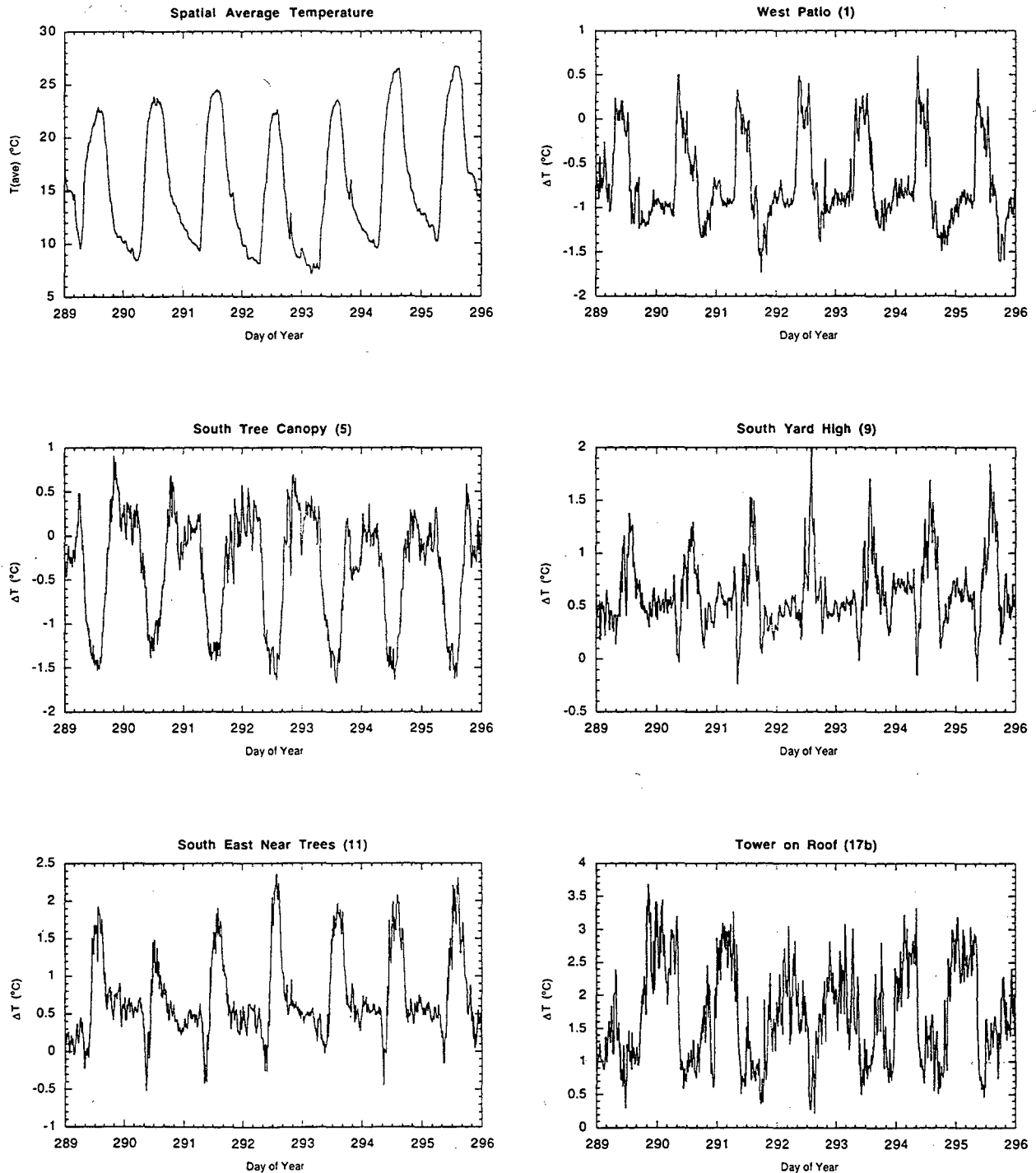
Figure 4. The spatial average temperature and subtractions. The sensors and time interval shown are the same as in Figure 3. Note the differing scales between the average, which is composed of the 13 sensors operating continuously through the experiment, and the temperature difference (sensor - average) for each of the sensors. The temperature-difference for each sensor roughly follows a diurnal pattern determined by the morphology of the sensor location.

33
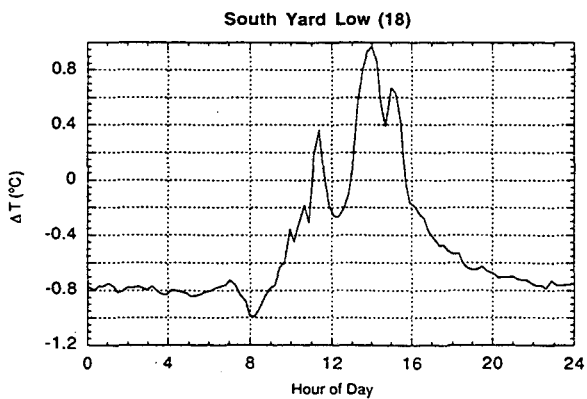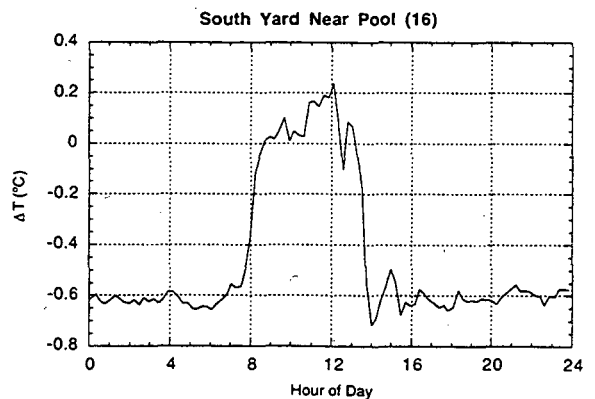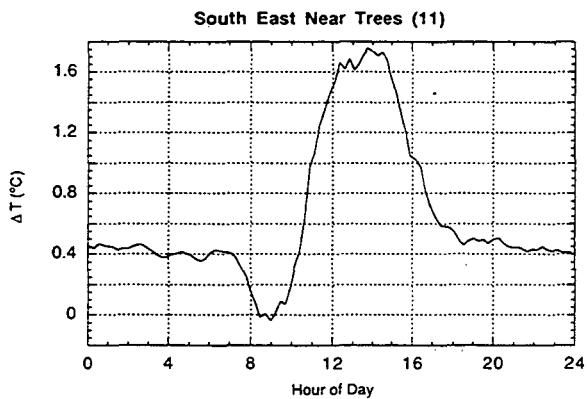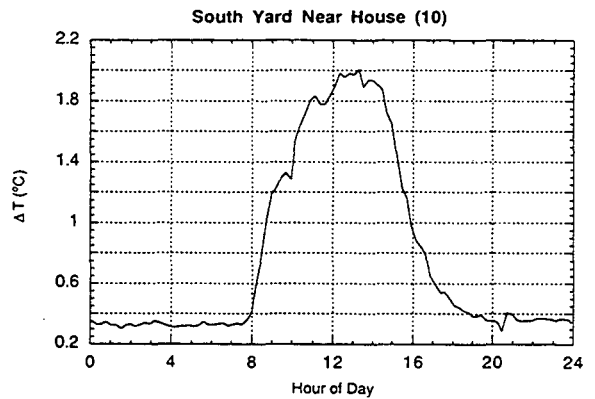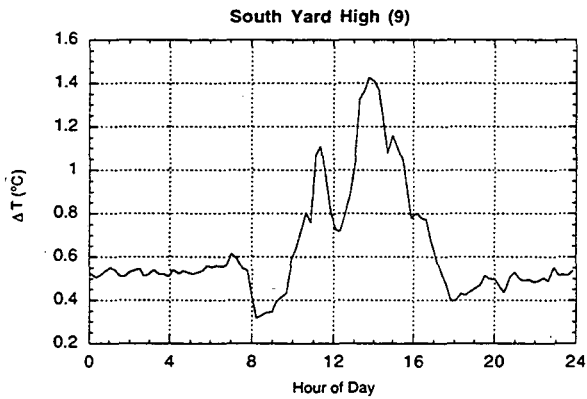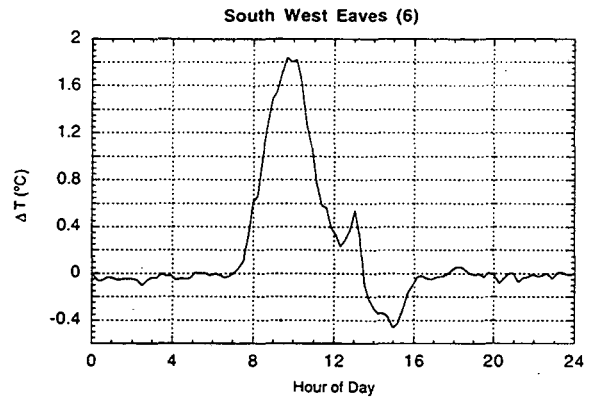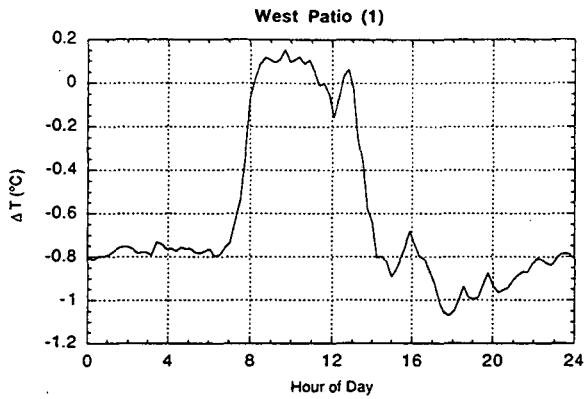
Figure 5a. Diurnal difference patterns of type I (single daytime maximum).
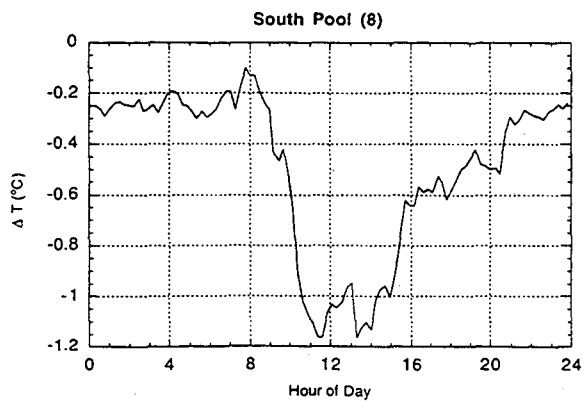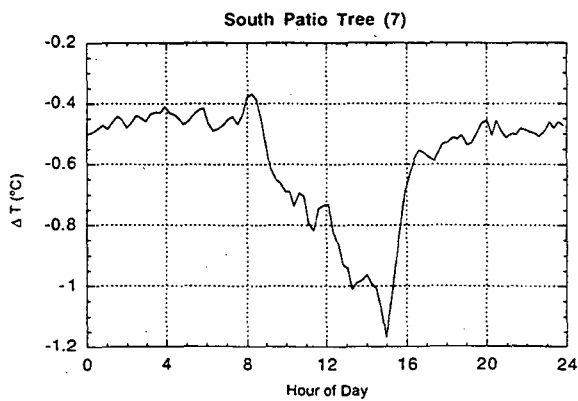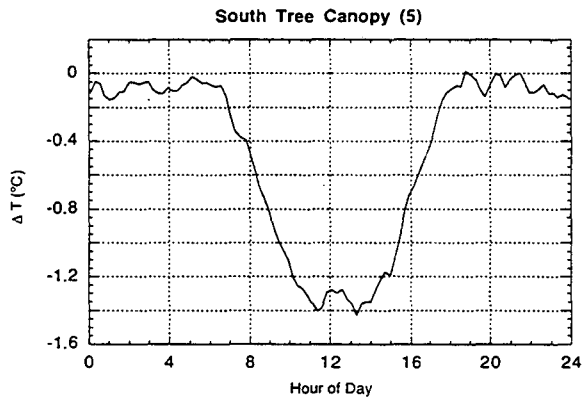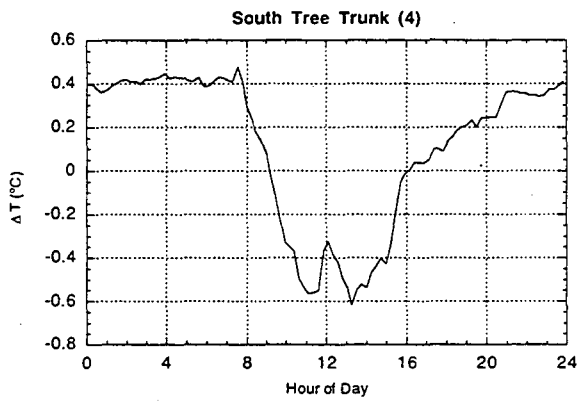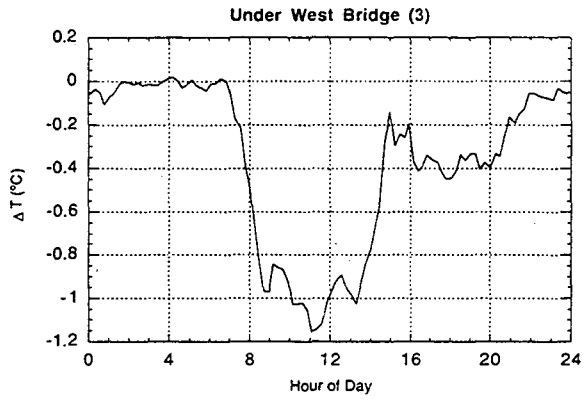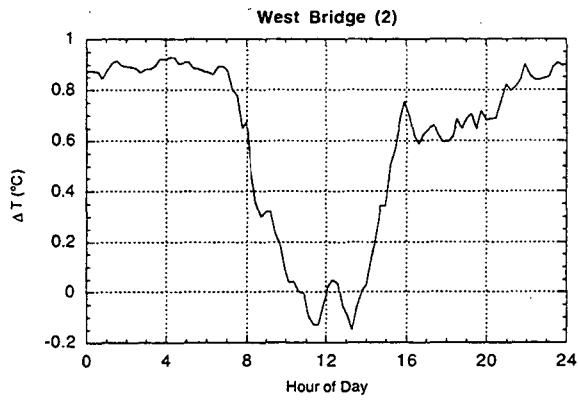
Figure 5b. Diurnal difference patterns of type II (single daytime minimum). (This and next page).

North East Tree (14)

North East Drive (15)

Roof Tower (17)

West Tree (19)

b. (con't.)

East Tree (13)
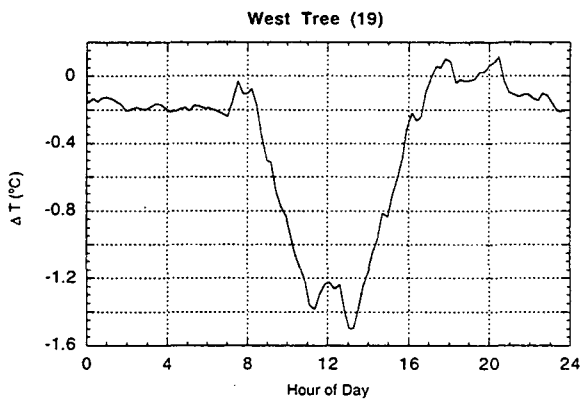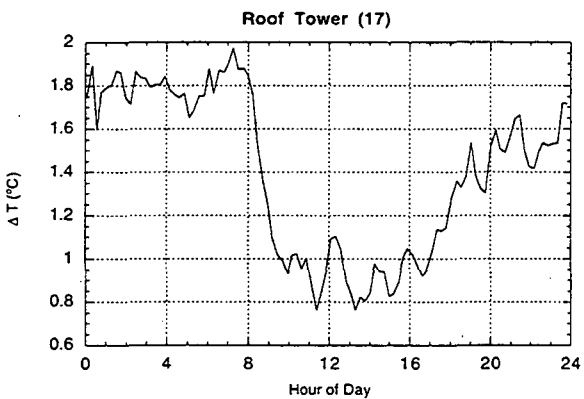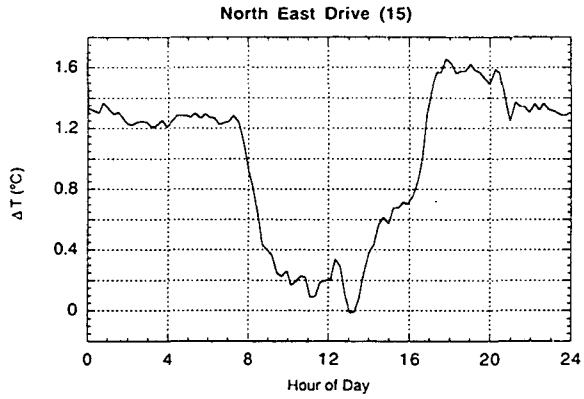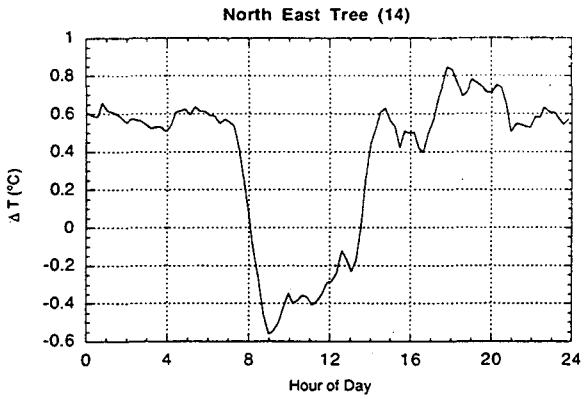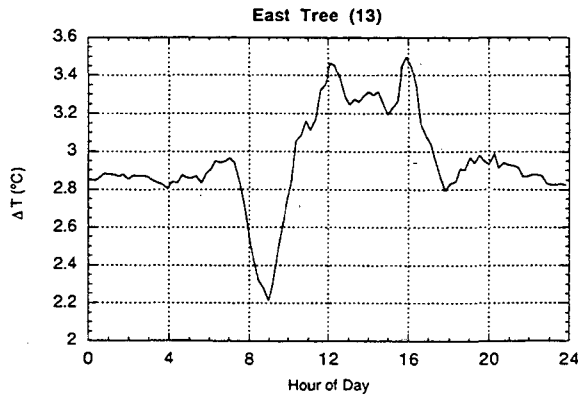
c.

Figure 5b (cont.) Diurnal patterns of type II.

Figure 5c. Diurnal difference patterns of type III (significant daytime minimum and maximum).

Insolation and Spacial Average Temperature

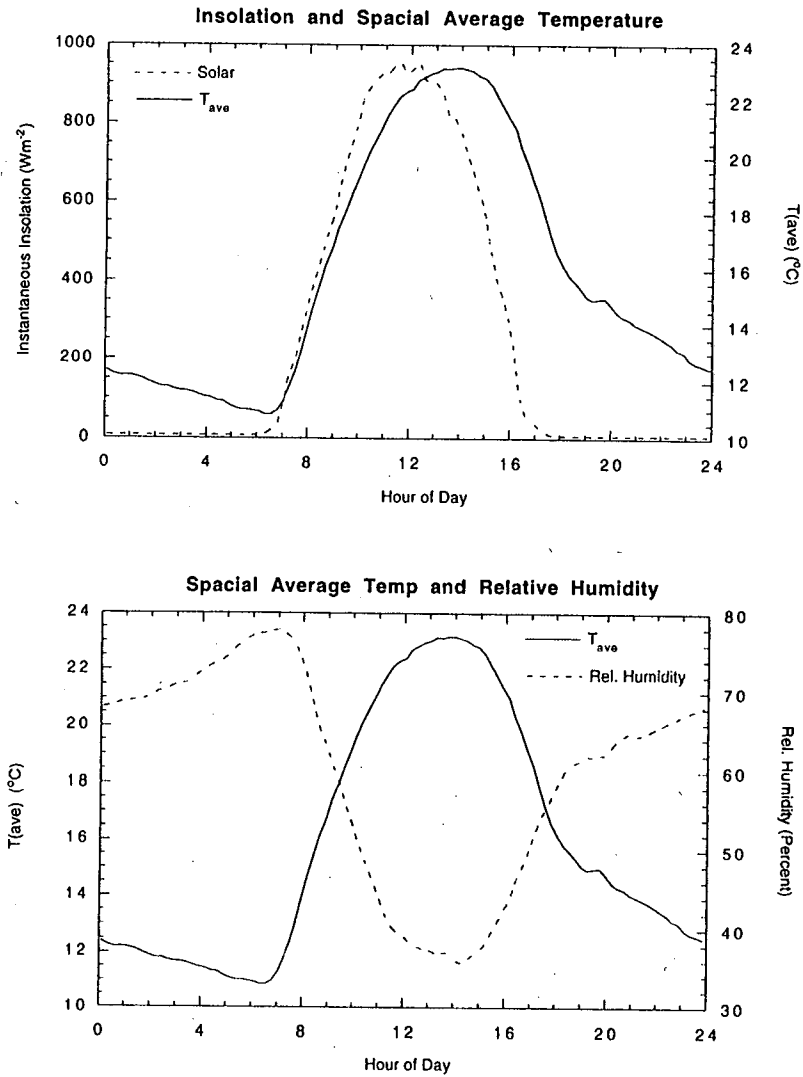

Spacial Average Temp and Relative Humidity

Figure 6. Diurnal patterns of climate variables; (a) Spacial average temperature begins to rise with isolation, but reaches a maximum 2 hours later, (b) Relative humidity tracks temperature as expected.

Daily Maximum of Average Temperature

Daily Maximum Insolation

Daily Maximum Relative Humidity
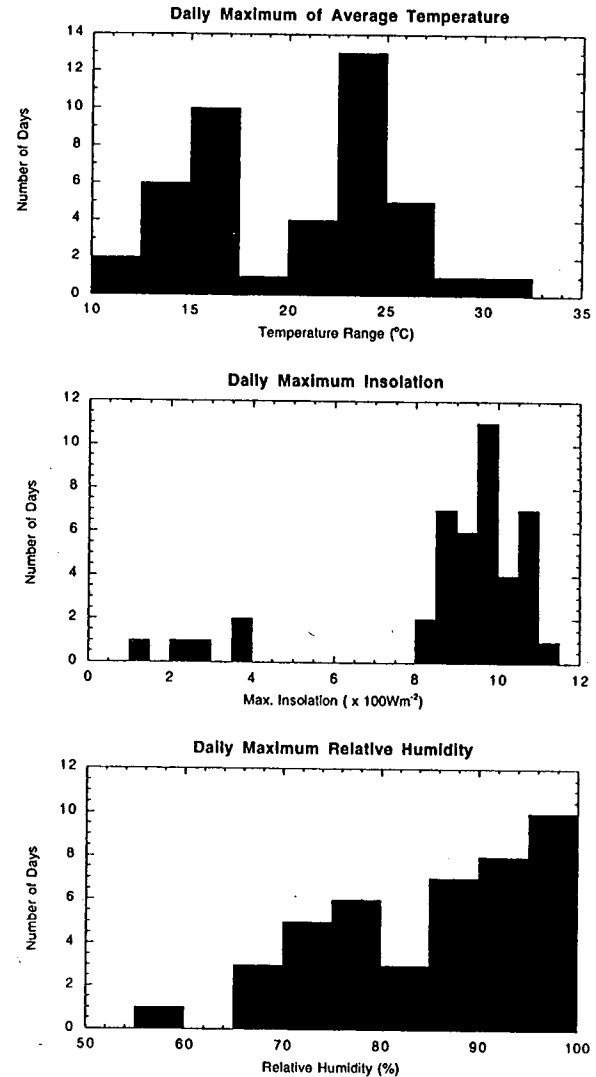

Figure 7. Distribution of synoptic climate variables over the interval covered in the analysis; (a) Temperature, (b) Insolation, (c) RH.

ERNEST ORLANDO LAWRENCE BERKELEY NATIONAL LABORATORY
ONE CYCLOTRON ROAD | BERKELEY, CALIFORNIA 94720